Geoscience Frontiers 5 (2014) 893–909

Contents lists available at ScienceDirect

China University of Geosciences (Beijing)

Geoscience Frontiers

journal homepage: www.elsevier.com/locate/gsf

Research paper

Sensitivity of digital elevation models: The scenario from two tropical mountain river basins of the Western Ghats, India

Jobin Thomas [a,*], Sabu Joseph [b], K.P. Thrivikramji [c], K.S. Arunkumar [d]

[a] Inter University Centre for Geospatial Information Science and Technology, University of Kerala, Thiruvananthapuram, Kerala, India
[b] Department of Environmental Sciences, University of Kerala, Thiruvananthapuram, Kerala, India
[c] Department of Geology, University of Kerala, Thiruvananthapuram, Kerala, India
[d] Department of Geology, MES College, Ponnani, Malappuram, Kerala, India

ARTICLE INFO

Article history:
Received 18 March 2013
Received in revised form
18 October 2013
Accepted 16 December 2013
Available online 11 January 2014

Keywords:
DEM
ASTER
SRTM
GMTED
Tropical mountain river basins
Western Ghats

ABSTRACT

The paper evaluates sensitivity of various spaceborne digital elevation models (DEMs), viz., Advanced Spaceborne Thermal Emission and Reflection Radiometer (ASTER), Shuttle Radar Topography Mapping Mission (SRTM) and Global Multi-resolution Terrain Elevation Data 2010 (GMTED), in comparison with the DEM (TOPO) derived from contour data of 20 m interval of Survey of India topographic sheets of 1: 50,000 scale. Several topographic attributes, such as elevation (above mean sea level), relative relief, slope, aspect, curvature, slope-length and -steepness (LS) factor, terrain ruggedness index (TRI), topographic wetness index (TWI), hypsometric integral (I_{hyp}) and drainage network attributes (stream number and stream length) of two tropical mountain river basins, viz., Muthirapuzha River Basin and Pambar River Basin are compared to evaluate the variations. Though the basins are comparable in extent, they differ in respect of terrain characteristics and climate. The results suggest that ASTER and SRTM provide equally reliable representation of topography portrayed by TOPO and the topographic attributes extracted from the spaceborne DEMs are in agreement with those derived from TOPO. Despite the coarser resolution, SRTM shows relatively higher vertical accuracy (RMSE = 23 and 20 m respectively in MRB and PRB) compared to ASTER (RMSE = 33 and 24 m) and GMTED (RMSE = 59 and 48 m). Vertical accuracy of all the spaceborne DEMs is influenced by relief of the terrain as well as type of vegetation. Further, GMTED shows significant deviation for most of the attributes, indicating its inability for mountain-river-basin-scale studies.

1. Introduction

On catchment scale, topography has a dominant control on hydrology and influences spatial distribution of various environmental factors, such as climate (Singh et al., 1995; Singh and Kumar, 1997; Bennie et al., 2008), soil formation (Jenny, 1941; Amundsen et al., 1994), soil moisture patterns (e.g., Western et al., 1999), soil properties (Chen et al., 1997; Johnson et al., 2000; Seibert et al., 2007) and even biodiversity (Florinsky and Kuryakova, 1996; Renfrew and Ribic, 2002; Zinko et al., 2005). For decades, topographic maps of varying scales have been used for the estimation of topographic attributes as well as in delineation of stream networks (Chapman, 1952; Pike and Wilson, 1971; Zevenbergen and Thorne, 1987), which is labor-intensive, expensive and time-consuming. Application of remote sensing and Geographic Information System (GIS) in earth-environmental-sciences and the developments in digital terrain analysis underscore digital elevation model (DEM) as an important component of hydrologic as well as geomorphologic research (e.g., Moore et al., 1992; Tarboton et al., 1992). Significant advances in remote sensing technology since its inception more than 50 years ago (Miller and Laflamme, 1958) have led to higher quality DEMs being generated by different techniques (contour-derived-, photogrammetric-, LIDAR- and RADAR-DEMs). Even though DEMs of differing spatial resolutions are freely

* Corresponding author. Tel.: +91 4712308214
E-mail address: jobinenv@gmail.com (J. Thomas).

Peer-review under responsibility of China University of Geosciences (Beijing)

Production and hosting by Elsevier

1674-9871/$ – see front matter © 2014, China University of Geosciences (Beijing) and Peking University. Production and hosting by Elsevier B.V. All rights reserved.
http://dx.doi.org/10.1016/j.gsf.2013.12.008

available (e.g., data of Advanced Spaceborne Thermal Emission and Reflection Radiometer, ASTER; Shuttle Radar Topography Mapping Mission, SRTM; Global Multi-resolution Terrain Elevation Data 2010, GMTED), choosing an appropriate data type for specific purposes still remains an enigma in geomorphologic and hydrologic applications (de Vente et al., 2009).

It is obvious that DEM errors adversely affect the accuracy and thereby modeling of natural processes (Lopez, 1997; Florinsky, 1998a). In addition, Vaze et al. (2010) demonstrated that the accuracy and resolution of the input DEM have serious implications on the hydrologically important spatial indices derived from the DEM. Hence, access of better quality input data is a major factor determining the successful application of environmental models at regional scale (Renschler and Harbor, 2002; Merritt et al., 2003). However, the only information regarding any global DEM provided is the global estimate of root mean square error (RMSE) and thus DEM accuracy at specific location needs to be estimated by the user. Several factors, such as source of data including collection techniques, location and density of samples, methods used for generation of DEM, spatial resolution and topographic complexity of the landscape affect the accuracy of DEM (Florinsky, 1998a; Thompson et al., 2001; Chaplot et al., 2006). Aguilar et al. (2005) suggested terrain morphology as the most important factor (compared to sampling density and interpolation techniques) determining the DEM accuracy. Compared to flatter terrains, mountainous topography has larger DEM errors contributed by terrain complexity, dense-vegetation-canopy and snow cover (Rodriguez et al., 2005; Nelson et al., 2009). However, recently, several researchers (e.g., Kervyn et al., 2008; Sharma et al., 2010; Prasannakumar et al., 2011; Darnell et al., 2012; Kia et al., 2012; Suwandana et al., 2012; Yamazaki et al., 2012; Zani et al., 2012; Elmahdy and Mostafa Mohamed, 2013) illustrated the expediency of spaceborne DEMs in geomorphometric and hydrologic applications in tropical environments.

In the regional context, Prasannakumar et al. (2011) demonstrated the suitability of SRTM data for geomorphometric analysis in parts of the Western Ghats, a prominent high-elevation passive margin with a well-defined escarpment extending for about 1500 km in NNW–SSE direction, parallel to the west coast of India (Ollier, 1990; Gunnell and Radhakrishna, 2001). Recently, Kale and Shejwalkar (2007, 2008), Magesh et al. (2011, 2013), Jayappa et al. (2012), Thomas et al. (2012) and Shinde et al. (2013) also employed either SRTM or ASTER data for various geomorphometric applications in various river basins draining the Western Ghats. However, hardly any attempt has been made to evaluate the accuracy and applicability of various spaceborne DEMs for geomorphometric and hydrologic applications in the tropical mountainous regions of the southern Western Ghats. Hence, this study is an outcome of comparing the sensitivity of various topographic attributes derived from different spaceborne DEMs (ASTER, SRTM and GMTED) with DEM generated from topographic contours (TOPO) of Survey of India (SoI) toposheets of 1:50,000 scale. In this study, we examine the DEMs to identify the most suitable DEM that can be used for geomorphometric and hydrologic applications in tropical mountainous terrain of the southern Western Ghats.

2. Study region

Two mountain river basins, viz., Muthirapuzha River Basin (MRB; area = 271.75 km^2, a sub-basin of west-flowing Periyar river) and Pambar River Basin (PRB; area = 288.53 km^2, a sub-basin of east-flowing Cauvery river) in the Anaimalai-Cardamom Hills of the southern Western Ghats have been selected for the investigation (Fig. 1). The basins are a part of the Precambrian high-grade Southern Granulite Terrain of the Peninsular India and the main rock types are hornblende-biotite-gneiss and granitoids. The drainage system of both MRB and PRB is influenced by the Munnar plateau (an extensive planation surface of late Paleocene age), and highest elevated surface (i.e., 1400 m above mean sea level, msl) in the southern Western Ghats (Soman, 2002). Thomas et al. (2010, 2011, 2012) emphasized the substantial influence of Munnar plateau in the development of the drainage characteristics of the basins. Several local planation surfaces (600–2200 m above msl) and terrain with concordant summits (2200–2400 m above msl) also characterize the region (Thomas et al., 2012). The basin elevation of MRB varies between 2690 (i.e., Anai Mudi, the tallest peak south of the Himalayas) and 760 m above msl, while that of PRB ranges from 2540 to 440 m above msl.

Even though tropical monsoon is the principal contributor of rainfall in the region, a distinguishable difference in climate exists between the basins due to distinctive terrain settings (Thomas, 2012). MRB is located on the western slopes of the southern Western Ghats and hence tropical humid climate (mean annual rainfall = 3700 mm, mean annual temperature = 17 °C), whereas PRB is on the eastern leeward slopes (and therefore rain shadow region with tropical semi-arid climate; mean annual rainfall = 1100 mm, mean annual temperature = 26 °C). MRB is covered by several natural vegetation belts including southern montane wet temperate grasslands, southern montane wet temperate forests (shola), west coast tropical evergreen forests and southern sub-tropical hill forests, while dominant vegetation types in PRB include southern montane wet temperate grasslands, southern montane wet temperate forests, southern tropical thorn forests, southern dry mixed deciduous forests and southern moist mixed deciduous forests. Tea and Eucalyptus plantations are common in both the basins.

3. DEM acquisition, characteristics and processing

This study makes use of four DEMs (of varying spatial resolution), viz., TOPO (derived from SoI toposheets), ASTER (http://earthexplorer.usgs.gov), SRTM (http://glcf.umiacs.umd.edu) and GMTED (http://eros.usgs.gov) to compare the topographic attributes for geomorphometric and hydrologic analyses as well as for landform characterization. In order to compare the applicability of the spaceborne DEMs, TOPO is taken as the reference DEM.

3.1. TOPO

The SoI topographic sheets (1: 50,000 scale) have been scanned with 750 dpi in TIFF format and georeferenced to real map coordinate system. Contours (of 20 m interval) as well as spot heights from topographic maps are vectorized in ArcGIS 9.3. To ensure data quality of the digital contour data, topology is created and various topology errors are corrected. The digitally captured contour elevation data is then converted to TOPO (with a spatial resolution of 20 m) using spatial analyst extension for ArcGIS 9.3 (Reuter and Nelson, 2009).

3.2. ASTER

The ASTER is an advanced multispectral imaging system of varying spatial resolution (15–90 m). ASTER consists of three different subsystems: the visible and near infrared (VNIR), the shortwave infrared (SWIR) and the thermal infrared (TIR), where VNIR (viz., Band 3-Nadir looking and Band 3-Backward looking; 0.76–0.86 μm) is the only one that provides stereo capability. ASTER relative DEM data has a horizontal accuracy of ±15 m and better and a vertical accuracy of ±15–25 m, depending on the environmental setting of the region. In an in-depth review, Toutin

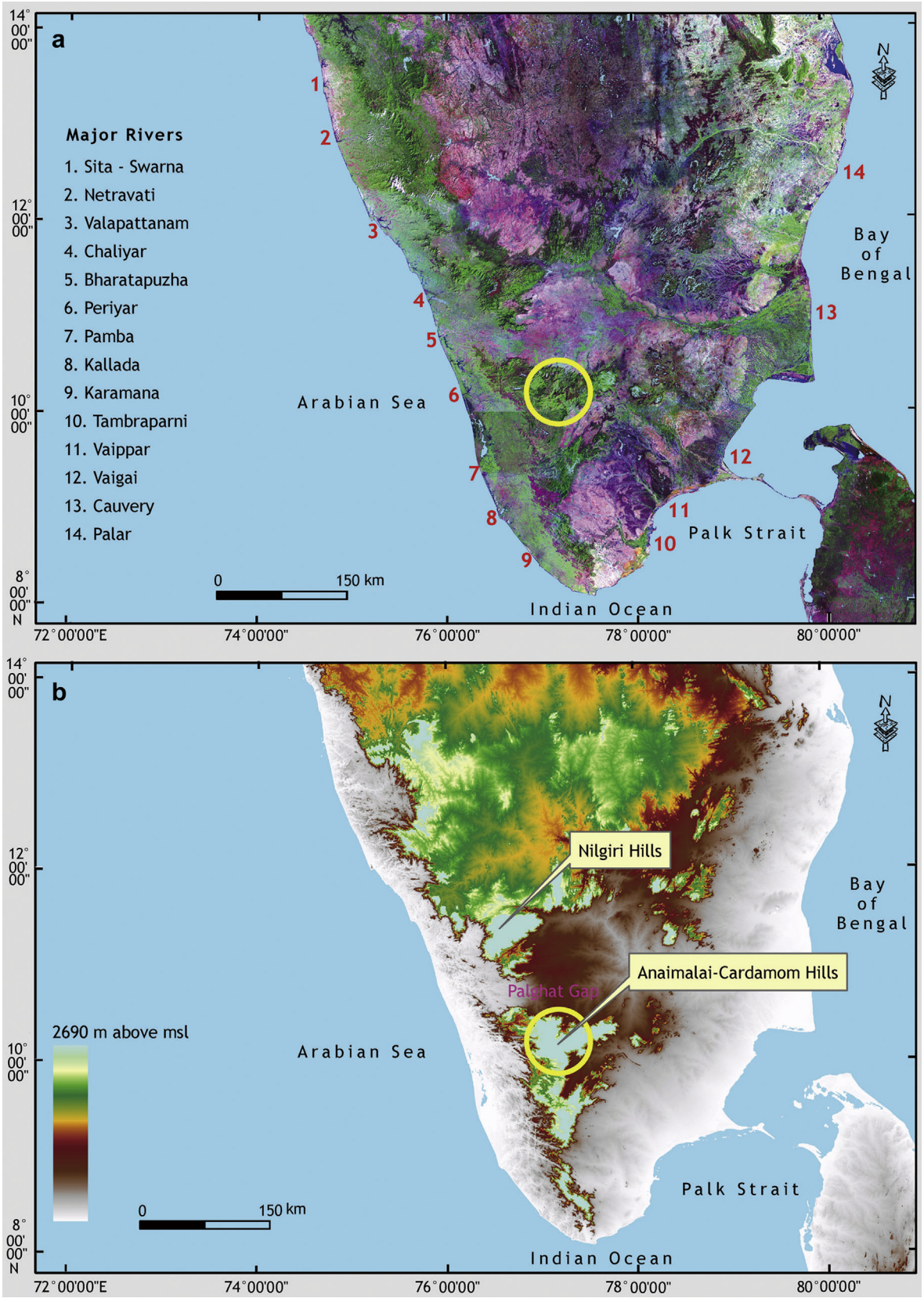

Figure 1. (a) Landsat image (Source: Global Land Cover Facility) and (b) SRTM 3 arc-second digital elevation data (Source: DEM Explorer) of southern India. Circle represents the area under investigation.

(2008) addressed the methods, algorithms and commercial software for generation of ASTER DEM and discussed the use of stereo ASTER DEMs for different geomatic and geoscientific applications.

3.3. SRTM

According to Rabus et al. (2003), SRTM generated the most complete high spatial resolution digital topographic database for the Earth using two antennas separated by a 60-m-long mast using C-band (5.6 cm wavelength) and X-band (3.1 cm wavelength) interferometric synthetic aperture radar (InSAR; Zebker and Goldstein, 1986). SRTM elevation data is readily available in three different resolutions, including 1 arc-second (30 m) resolution for the US and 3 arc-seconds (90 m) and 30 arc-seconds (1 km) resolutions for rest of the mapped landmass of the world. The linear vertical relative height error and circular relative geolocation error of the SRTM data is less than 10.0 and 15.0 m respectively for 90% of the data. SRTM data is referenced to the WGS84-EGM96 geoid and is georeferenced in the horizontal plane to the WGS84 ellipsoid. SRTM DEM represents a digital surface model (DSM), which is influenced by natural and man-made features and hence provides heights of the earth's surface including topographic objects such as buildings, vegetation etc. (Nelson et al., 2009). More elaborate details and reviews of SRTM datasets including issues such as accuracy, errors, applications etc. are given in Rodriguez et al. (2006), Slater et al. (2006), Farr et al. (2007), Jarvis et al. (2008) and Kervyn et al. (2008).

3.4. GMTED

GMTED is a suite of seven raster data products, viz., minimum elevation, maximum elevation, mean elevation, median elevation, standard deviation of elevation, systematic subsample and breakline emphasis (Danielson and Gesch, 2011). The spatial resolution of GMTED ranges from 30 arc-seconds (1 km), 15 arc-seconds (500 m) and 7.5 arc-seconds (250 m).

4. GIS analysis

The DEMs are reprojected into Universal Transverse Mercator (zone 43) projection for the analyses. The DEMs used in this study are from different sources and of varying spatial resolutions (i.e., TOPO–20 m, ASTER–30 m, SRTM–90 m and GMTED–250 m). In order to compare the raster datasets, there is a need for rescaling of the DEMs in that all the DEMs should be resampled to a common spatial resolution (Nikolakopoulos et al., 2006; Prasannakumar et al., 2011). Here, a pixel resolution of 90 m is set as the spatial scale for analysis and all the DEMs have been resampled to 90 m. Among various resampling techniques, bilinear interpolation method is used in this study, which determines the new value of a cell based on a weighted distance average of the four nearest input cell center points. Further, a low pass filter with 3 × 3 kernel neighborhood has been applied to all the resampled DEMs to improve the quality by removing spurious data/outliers in the data. Co-registration of the DEMs is essential to remove the potential horizontal and vertical shifts between input DEMs before analysis. The spaceborne DEMs have been co-registered to the coordinate system of TOPO based on 20 ground control points (GCPs) collected from the input DEMs. From the processed DEMs, various topographic attributes, viz., relative relief, slope, aspect, curvature (profile and plan), slope-length and -steepness (LS) factor, terrain ruggedness index (TRI), topographic wetness index (TWI) and hypsometric integral (I_{hyp}) have been derived (Suppl Tables). Various landforms are characterized according to a rule-based classification regime after Weiss (2001) and Jenness (2006).

All the DEMs are corrected for hydrologic analysis by creating a seamless elevation grid without any sinks for each basin. Sink occurs when all neighboring cells are higher than the processing cell, which has no downslope flow path to a neighbor cell. Occasionally sinks could be real components of the terrain, but are also the result of input errors or interpolation artifacts generated during DEM production or resampling process (Wu et al., 2008). Hence, the sinks have been removed by grid filling function to ensure proper delineation of stream network. Further, flow direction (using D8 flow algorithm) and flow accumulation have been estimated and cells with flow accumulation higher than a threshold value are identified as stream networks. The threshold value represents the minimum upstream drainage area necessary to maintain a stream and hence the number and total length of streams as well as the order of the basin (and thereby basin morphometry) strongly depend on the threshold value. Several studies, e.g., Quinn et al. (1995), Gandolfi and Bischetti (1997) demonstrated that the choice of different threshold values may influence the accuracy of stream network parameters. Since one of the purposes of this study is to compare drainage networks derived from various DEMs, but with same resolution, a common threshold of 100 cells is applied to derive stream networks. Further the derived stream networks are ordered after Strahler (1957) and bifurcation ratio and drainage density (Horton, 1945) of the basins have been calculated (Suppl Fig.).

5. Results

5.1. Assessment of DEM accuracy

The vertical accuracy in elevation among different DEMs (TOPO, ASTER, SRTM and GMTED) is assessed by comparing elevation data derived from different DEMs with the elevation data of the reference points. Even though TOPO is the reference DEM, it also contains interpolation errors. According to the National Geospatial Programme Standards and Specifications for the collection, processing and quality control of DEMs (USGS, 1998), minimum number of 28 test points per DEM is required (20 interior points and 8 edge points) to verify the accuracy of a DEM (Greenwalt and Shultz, 1962). In addition, Reuter et al. (2009) suggested that the reference points should be (a) evenly distributed across the area of interest, (b) representative of the landscape and (c) measured to a much higher precision than the DEMs being tested. Hence, this study also makes use of 28 test points (i.e., surveyed benchmark points) for each DEM to assess the vertical accuracy. Even though there are several approaches to estimate the errors in DEM data, mean absolute error (MAE) and RMSE are the most widely used error statistics (Eqs. (1) and (2)).

$$\mathrm{MAE} = \frac{1}{n}\sum_{i=1}^{n}|\mathrm{REF}_i - \mathrm{DEM}_i| \tag{1}$$

$$\mathrm{RMSE} = \sqrt{\frac{1}{n}\sum_{i=1}^{n}(\mathrm{REF}_i - \mathrm{DEM}_i)^2} \tag{2}$$

where, REF_i is the reference elevation of ith location, DEM_i is the elevation obtained from DEM for ith location, $\overline{\mathrm{REF}}$ is the mean of the reference elevations of all locations and n is the total number of sample locations.

Although MAE provides a more detailed evaluation of the DEM error, it gives little insight into their spatial distribution. Since RMSE is closely associated with DEM data generation techniques and accounts for both random and systematic errors introduced during

the data generation process, it is widely used as an overall indicator for vertical accuracy assessment of DEMs (Nikolakopoulos et al., 2006; Reuter et al., 2009; Hirt et al., 2010; Mouratidis et al., 2010). Estimated MAE and RMSE of different DEMs of MRB and PRB are given in Table 1.

Even though all the DEMs of MRB and PRB show a significant linear relationship with corresponding reference elevation data (Fig. 2), TOPO shows relatively higher vertical accuracy which manifests as lower MAE and RMSE (8.0 and 9.0 m in MRB; 9.0 and 10.0 m in PRB). According to SRTM mission specifications, vertical accuracy of SRTM DEM data is ±16.0 m, whereas results of this study show comparatively larger errors (i.e., 23 m for MRB and 20 m for PRB; Table 1). Similarly, depending on the environmental setting of the region, vertical accuracy of ASTER DEM varies between 15 and 25 m. However, vertical accuracy of ASTER DEM of MRB is well outside the range (Table 1). In addition, GMTED data of MRB and PRB (59 and 48 m, respectively) are also significantly higher than the theoretical values (26–30 m). The variation in the vertical accuracies of the spaceborne DEMs could be attributed to the topographic complexity of the terrain under investigation.

5.2. Comparison of topographic attributes

Suppl Tables are a statistical summary of topographic attributes used in the study for comparing the DEM datasets.

5.2.1. Elevation

The TOPO, ASTER, SRTM and GMTED DEMs of MRB and PRB are given in Figs. 3 and 4. The minimum elevation of MRB extracted from TOPO is 740.81 m above msl (Suppl Tables), whereas that of ASTER, SRTM and GMTED is 741, 746 and 772 m above msl respectively. Similarly, in PRB, minimum elevation obtained from TOPO is 440 m above msl, while ASTER and SRTM DEMs give comparatively lower elevation (434 and 437 m above msl) and GMTED provides relatively higher elevation (449 m above msl). However, in both the basins, the maximum elevation values show relatively larger variation compared to the minimum elevation (Suppl Tables). In MRB, TOPO registers a maximum elevation of 2685.29 m above msl, whereas other DEMs have values in the range of 2614 (ASTER) to 2638 m above msl (SRTM). Likewise, maximum elevation of PRB obtained from TOPO is 2540 m above msl, while other DEMs give relatively lower values, e.g., 2526 (ASTER), 2530 (SRTM) and 2511 (GMTED) above msl respectively. However, there is only a minor variation in mean elevation of the basins derived from TOPO, ASTER and SRTM (<0.15% in MRB and <0.50% in PRB). Even though mean elevation of the basins derived from GMTED is relatively larger, the deviation is under one percent.

Further, in either basins, SRTM shows better agreement with elevation range of TOPO. Several studies in different geographic areas (e.g., Pryde et al., 2007; Hirt et al., 2010; Suwandana et al., 2012) showed that ASTER DEM (with a pixel size of 30 m) has relatively lower elevation accuracy than SRTM, even if the latter has a relatively coarser resolution (i.e., 90 m). Moreover, Suwandana et al. (2012) observed a better association between TOPO and SRTM (rather than ASTER) in headwater areas, where elevation reaches nearly 1900 m above msl. However, mean elevation of MRB derived from ASTER and TOPO also shows hardly any large differences. The cumulative area curves, representing the spatial distribution of elevation in relation with their areal extent, of MRB and PRB (Fig. 5a,b) do not show significant variations, implying the comparability of the spaceborne DEMs with TOPO. In both the basins, the only noticeable variation in the distribution of elevation among the DEMs is in the range >2000 m above msl. The distribution of elevation of MRB and PRB significantly differs, which is resulted from the contrasting terrain settings and all the DEMs clearly picturize the characteristic topographic profile irrespective of their spatial resolution.

Table 1
Error statistics of various DEMs of MRB and PRB.

	MRB				PRB			
Error statistics	TOPO	ASTER	SRTM	GMTED	TOPO	ASTER	SRTM	GMTED
MAE (m)	8	28	19	47	9	21	17	44
RMSE (m)	9	33	23	59	10	24	20	48

5.2.2. Relative relief

The variability in elevation across a basin can be represented simply as the difference in maximum and minimum elevations (i.e., local relief) or as a better measure, local relief normalized by area (i.e., relative relief) and either geomorphometric indices provide sufficient information regarding the general topography. Relative relief standardizes the change in elevation over an area and hence a useful measure of ruggedness for river basin comparisons. In this study, spatial variation of relative relief (in m/km^2) has been generated from the DEMs using the range function of neighborhood statistics available in the Spatial Analyst extension of ArcGIS 9.3.

In MRB, the range of relative relief values (in m/km^2) derived from TOPO is between 40.88 and 703.78 (mean = 275.89). Even though other DEMs also show significant variations (i.e., range = 62–688 from ASTER, 56–725 from SRTM and 26–724 m from GMTED), the mean relative relief of the DEMs (ASTER = 270.01; SRTM = 270.18) except GMTED (241.62) is very close to that of TOPO (275.89; Suppl Tables). Similarly, in PRB also, the mean of relative relief of ASTER and SRTM (332.06 and 331.46 m/km^2 respectively) is comparable with that of TOPO (334.07), while GMTED shows a relatively lower mean (304.92). In both the basins, the spatial variation of relative relief with respect to their areal coverage derived from ASTER and SRTM is similar to that of TOPO. However, GMTED overestimates the relative relief especially in areas of lower relative relief, e.g., 600 m/km^2 (Fig. 5c,d).

5.2.3. Slope

Slope (the rate of change of elevation in the direction of steepest descent) has significant influence on the velocity of surface and subsurface flow, soil water content, erosion potential, soil formation and several other earth surface processes (Gallant and Wilson, 2000) and hence an important parameter in hydrologic and geomorphologic studies.

The slope (in degree) distribution in MRB and PRB derived from various DEMs is summarized in Suppl Tables. In MRB, the range of slope derived from ASTER (0.23–60.37) and GMTED (0.00–62.08) shows better similarity with that of TOPO (0.00–63.60), while the slope of SRTM shows a relatively narrow range (i.e., 0.00–56.91). However, in PRB, the range of slope provided by SRTM (0.11–63.69) is significantly closer to that of TOPO (0.00–66.01), whereas ASTER underestimates the slope (0.11–58.38) and GMTED shows an overestimated range (0.00–72.53). In the case of GMTED, the overestimated slope values are mainly observed in areas having slope <20°. In MRB and PRB, the spatial distribution of slope with respect to the areal coverage has significant comparability among TOPO, ASTER and SRTM (Suppl Tables; Fig. 6a,b) and the areal coverage of various slope classes is more or less uniform for the ASTER and SRTM (Suppl Tables).

5.2.4. Aspect

Aspect (the orientation of the line of steepest descent) is an anisotropic topographic attribute, i.e., depends on a specific geographical direction, such as to the Sun's azimuth (Zevenbergen

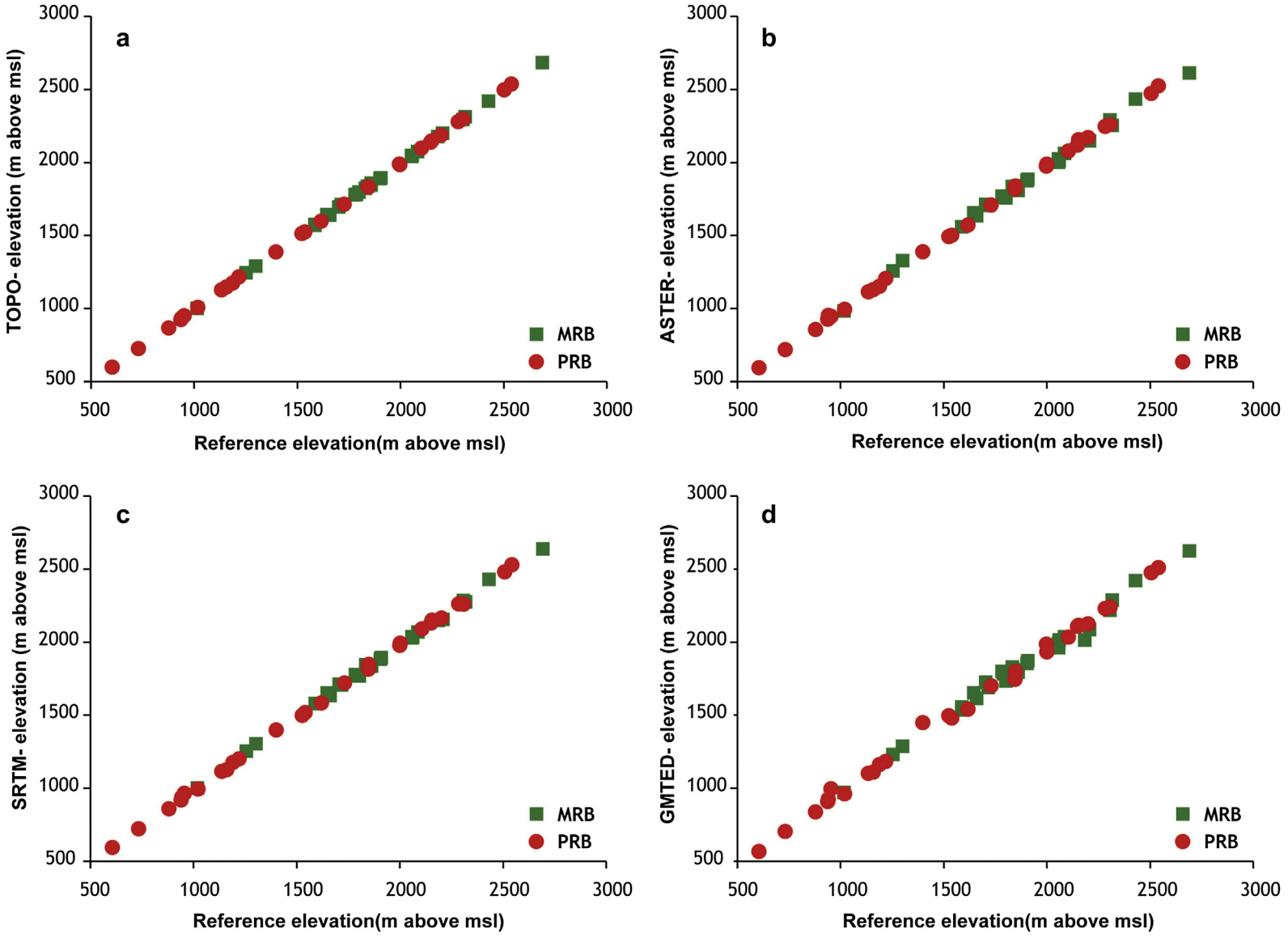

Figure 2. Scatter plot of reference elevation vs. elevation from (a) TOPO, (b) ASTER, (c) SRTM, and (d) GMTED of MRB and PRB.

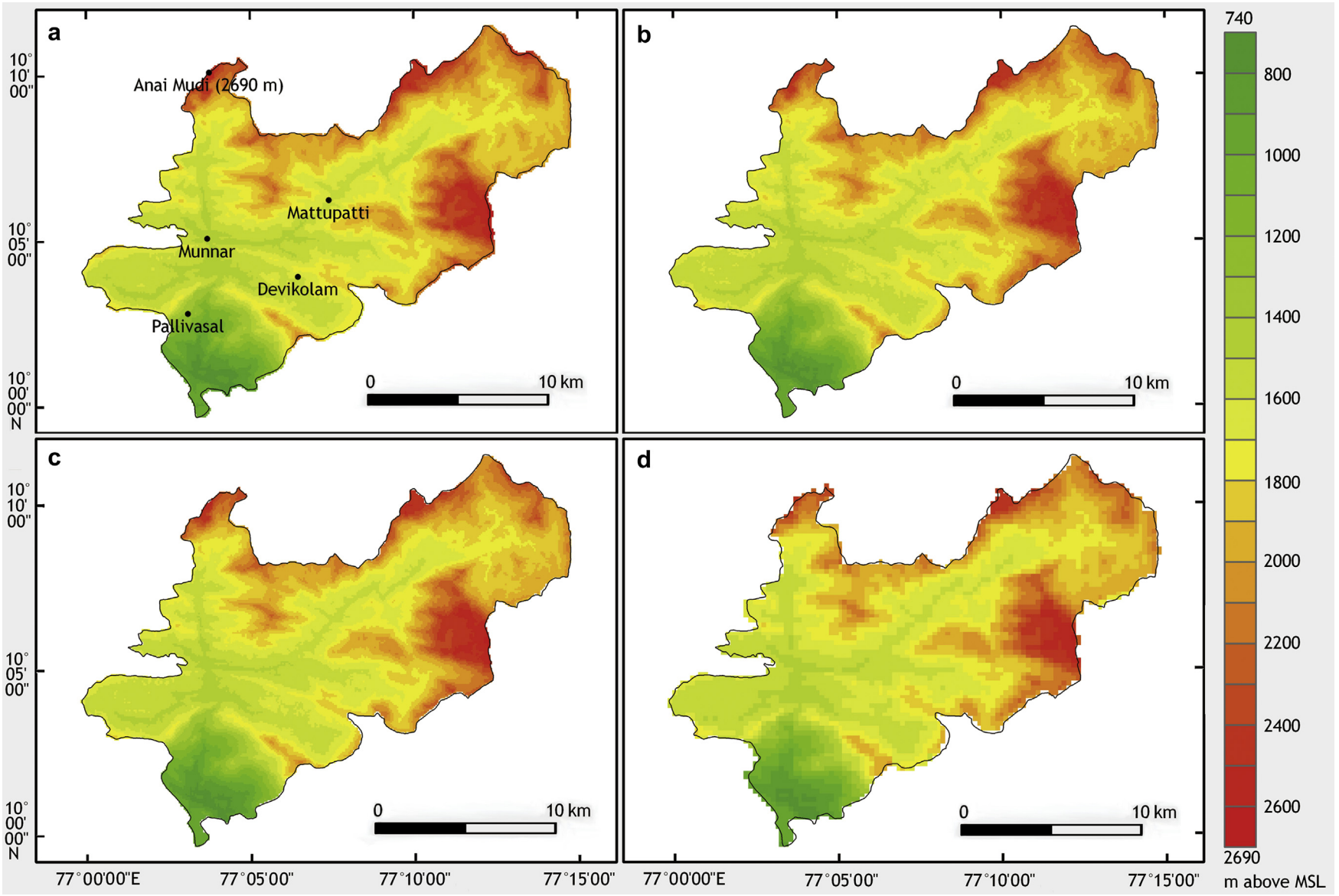

Figure 3. DEMs of MRB (a) TOPO, (b) ASTER, (c) SRTM and (d) GMTED.

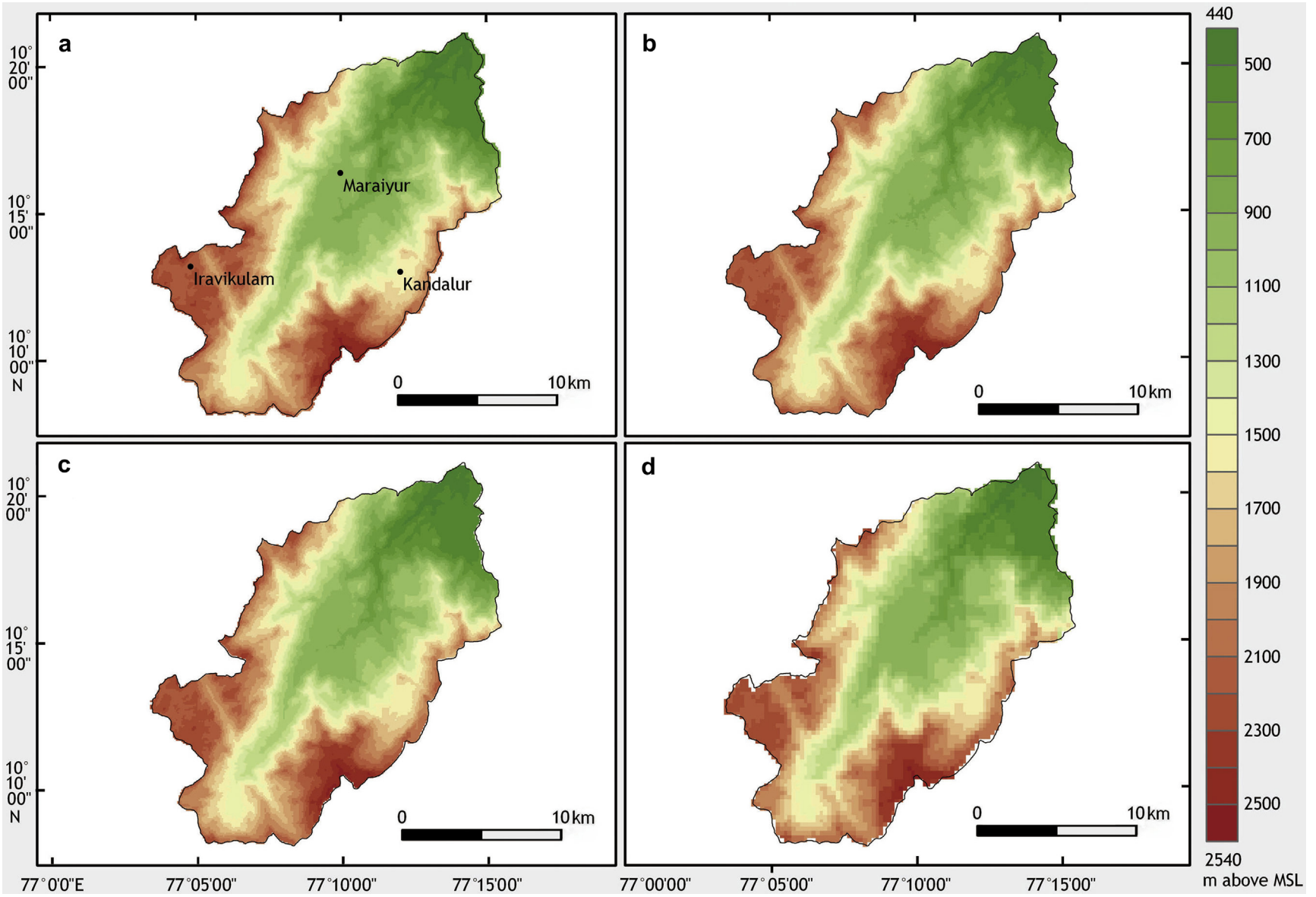

Figure 4. DEMs of PRB (a) TOPO, (b) ASTER, (c) SRTM and (d) GMTED.

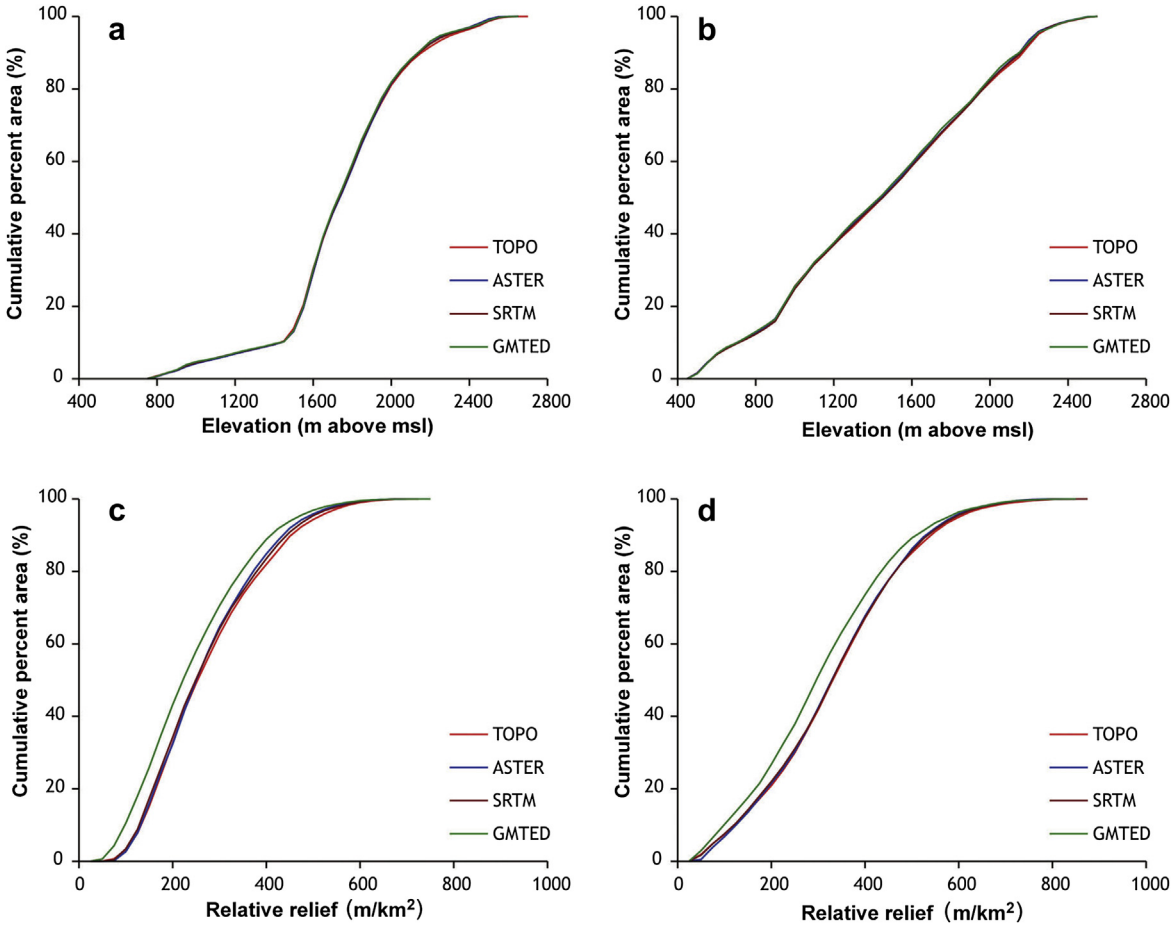

Figure 5. Cumulative frequency distributions for (a) elevation, MRB, (b) elevation, PRB, (c) relative relief, MRB and (d) relative relief, PRB.

and Thorne, 1987). Aspect measures in degrees clockwise from north and an aspect value of −1 is generally assigned for flat areas. It has a significant influence on the distribution of vegetation, biodiversity and agricultural productivity because solar radiation received at a location on the terrain depends on the aspect and shadows cast by terrain.

Even though aspect maps generated from TOPO, ASTER, SRTM and GMTED show significantly similar range of values for both the basins, mean aspect derived from GMTED (157.54 and 139.66 respectively for MRB and PRB) is numerically lower than other DEMs (Suppl Tables). In order to understand the reasons for such an anomalous behavior of GMTED, areal extent of each aspect is measured (Suppl Tables) and the results suggest that GMTED shows an overestimation (in the order of magnitude) of areal coverage for flat areas, which significantly reduced mean aspect of the basins. In MRB, on comparison of areal coverage of various aspects, SRTM shows a better similarity with TOPO compared to ASTER, whereas in PRB, N, NE, S and NW aspects of TOPO and SRTM show better agreement, while E, SE, SW and W match with ASTER (Suppl Tables).

5.2.5. Curvature

The curvature of a topographic surface is mostly expressed in terms of profile and plan curvature, where the former is the curvature of a surface in the direction of the slope and the latter is the surface curvature perpendicular to the direction of slope. Profile curvature - positive for a convex surface and negative for concave - measures the rate of change of slope and therefore influences the flow velocity of water draining the surface, which in turn controls erosion and deposition. Plan curvature or contour curvature is the curvature of a "hypothetical" contour line passing through the cell (line formed by intersection of a horizontal plane with the terrain). Plan curvature is positive for convex-outward, negative for concave-outward surfaces and controls the convergence or divergence of water (Zevenbergen and Thorne, 1987).

In MRB, profile curvature of TOPO varies between −3.63 and 2.80 (Suppl Tables), while ASTER (−2.00 to 2.25) and SRTM (−2.87 to 2.71) provide a relatively narrow range. However, GMTED has a comparatively larger range compared to other DEMs (−4.40 to 4.40). Similarly, in PRB, ASTER and SRTM have comparatively lower range of profile curvature (−2.40 to 2.38 and −3.66 to 2.82 respectively) and GMTED with relatively higher (−7.35 to 7.35), with respect to TOPO (−3.62 to 3.11). However, mean profile curvature of SRTM is identical to that of TOPO in MRB and PRB (0.015 and 0.010 respectively). The range of plan curvature of MRB derived from TOPO ranges from −1.56 to 2.43 (Suppl Tables), while ASTER and SRTM show range of values from −1.32 to 1.56 and −1.95 to 3.37 respectively. In PRB, plan curvature of TOPO is between −2.22 and 3.01, whereas the values range from −1.52 to 1.65 and −2.71 to 3.53 respectively for ASTER and SRTM. GMTED provides relatively larger range of plan curvature in MRB and PRB (−4.02 to 3.79 and −5.23 to 5.85 respectively). Similar to profile curvature, mean of plan curvature derived from SRTM show identical values (with respect to TOPO) in MRB and PRB (Suppl Tables). Even though the range of curvature for various DEMs shows salient differences, majority of the data cluster between −1.0 and +1.0.

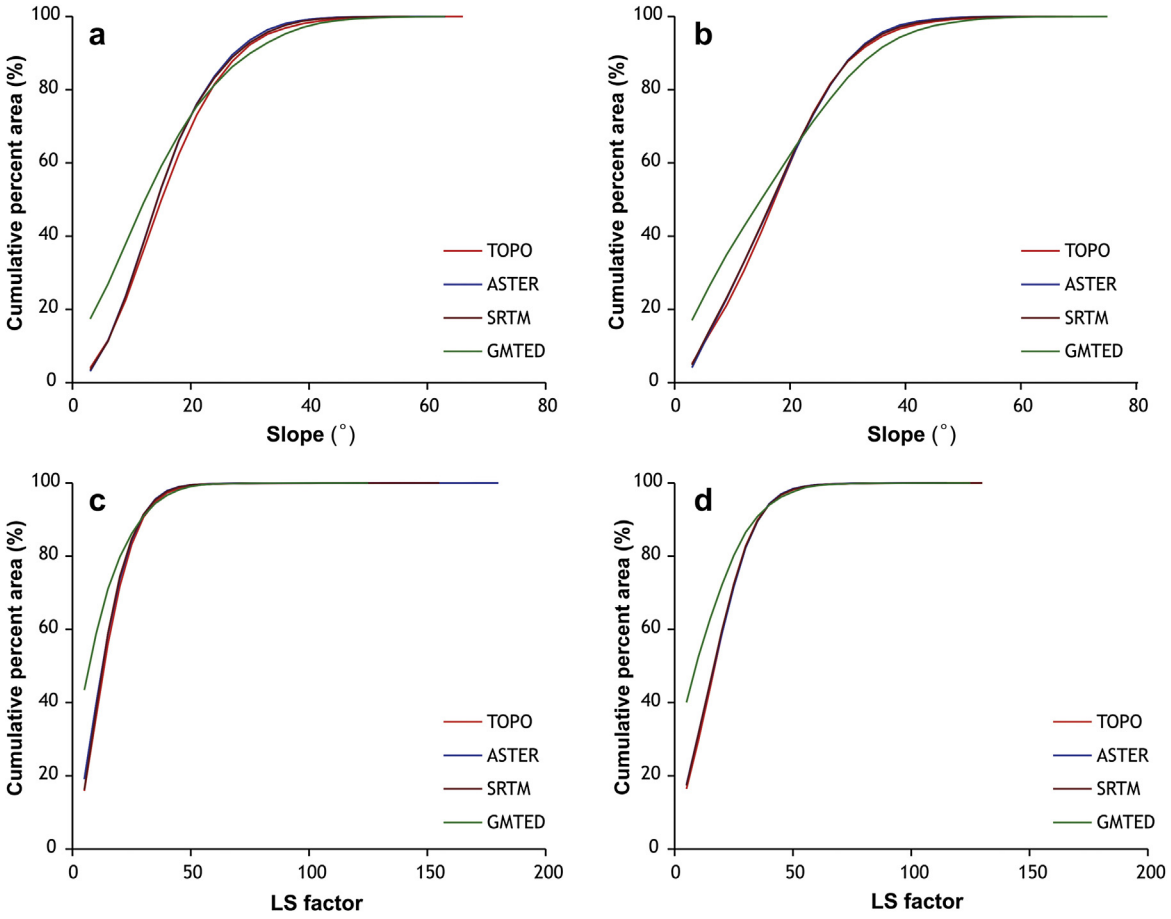

Figure 6. Cumulative frequency distributions for (a) slope, MRB, (b) slope, PRB, (c) LS factor, MRB and (d) LS factor, PRB.

5.2.6. LS factor

The LS (or topographic) factor, derivative of unit stream-power theory (Moore and Burch, 1986a, b), is one of the parameters in empirical soil erosion models such as Universal Soil Loss Equation (USLE) and its modified and revised forms to incorporate the influence of topography on soil loss (Wischmeier and Smith, 1978; Renard et al., 1997). It calculates a spatially distributed sediment transport capacity that has significant implications in landscape assessment because it explicitly accounts for flow convergence and divergence (Moore and Wilson, 1992). A modified form of LS factor is occasionally used to predict areas of net erosion and net deposition (Wilson and Gallant, 2000).

In MRB and PRB, the range of LS factor derived from TOPO and SRTM (0–153 in MRB and 0–129 in PRB) is co-varying, while ASTER and GMTED show considerable deviation from the range (Suppl Tables). In MRB, ASTER has a relatively wider range (0–177), while a comparably narrow range (0–122) has been generated by GMTED. In PRB, ASTER and GMTED show numerically smaller range of values (0–112 and 0–122 respectively). Even though mean LS values of ASTER and SRTM do not vary significantly compared to TOPO, GMTED provides relatively lower LS factors (Suppl Tables). The geometry of spatial distribution curves of LS factor derived from the DEMs (except GMTED) is more or less uniform in either the basins (Fig. 6c,d).

5.2.7. Terrain ruggedness index (TRI)

In general, most of the geomorphologic research expresses terrain heterogeneity in qualitative terms such as undulating, broken, rugged or dissected and often measures in terms of surrogate variables, such as dissection index, drainage density etc. However, it is an important variable for predicting environment specific habitat location and species density (Koehler and Hornocker, 1989; Fabricius and Coetzee, 1992). Estimates of terrain heterogeneity have been mostly calculated using labor-intensive techniques or techniques designed for specific areas (Beasom et al., 1983; Fabricius and Coetzee, 1992; Nellemann and Fry, 1995). Later, Riley et al. (1999) developed TRI (a derivative of DEM) using a terrain analysis function and provided a rapid, objective measure of terrain heterogeneity, which is used in this study to assess the ruggedness of terrain.

In MRB, TRI of TOPO is in the range of 18–363 (Suppl Tables), whereas varying ranges have been yielded by ASTER (19–323), SRTM (15–316) and GMTED (14–298). Mean TRI values of the spaceborne DEMs are also far below than that of TOPO. However, in PRB, the mean and the range of TRI of SRTM (mean = 119.13; range = 9–410) are very much closer to TOPO (mean = 120.78, range = 10–430). Although the range of TRI of ASTER (10–387) and GMTED (10–455) shows distinct differences compared to TOPO and SRTM, the mean values of the DEMs have meager variability (Suppl Tables). GMTED slightly overestimates TRI in areas which are either level or slightly rugged (i.e., TRI < 161).

5.2.8. Topographic wetness index (TWI)

The TWI is defined as ln (a/tanβ) where 'a' is the local upslope area draining through a certain point per unit contour length and tanβ is the local slope (Beven and Kirkby, 1979). One reason the TWI has been so successful is that it represents an objective way to

parameterize first-order controls on water movement from topographic information (Hjerdt et al., 2004). TWI is related to several landscape attributes such as flow accumulation, soil moisture, distribution of saturation zones, depth of water table, evapotranspiration (Beven and Kirkby, 1979; Quinn and Beven, 1993), thickness of soil horizons, organic matter, pH, silt and sand content (Moore et al., 1993), vegetation distribution (Florinsky and Kuryakova, 1996) and erosion potential (Burt and Butcher, 1985).

In MRB, the mean and range of TWI derived from ASTER are identical to that of TOPO (mean = 11.78, range = 8–26; Suppl Tables). Even though TWI of SRTM also exhibits the same range, mean TWI is relatively smaller (compared to TOPO and ASTER). Similarly, in PRB, TOPO and ASTER have a common TWI range (8–26; Suppl Tables). Although SRTM has a different range of TWI (7–26), mean TWI (11.82) is relatively closer to TOPO (11.91) than that of ASTER (11.79).

5.2.9. Landform characterization

Classification of terrain into various geomorphic classes (or landforms) is very essential for comprehensive river basin planning and management. The topographic analysis tool (after Jenness, 2006) for ArcGIS 9.3 is used for the landform classification. Based on the topographic attributes, grid cells are classified into either 10 of the different landform classes, viz., (1) deeply incised valley, (2) mid-slope shallow valley, (3) headwaters, (4) U-shaped valleys, (5) plains, (6) open slopes, (7) upper slopes/mesa, (8) local ridges/hills in valleys, (9) mid-slope ridges/smaller hills in plains and (10) high ridges/mountain top. The areal coverage of various landforms of MRB and PRB is depicted in Fig. 7a,b.

A detailed investigation on the areal extent of various landforms clearly suggests that none of the spaceborne DEMs, viz., ASTER, SRTM and GMTED exactly classify the landforms as the TOPO does. The landform classes of TOPO show varying levels of similarity with landforms derived from other DEMs. For example, in MRB, landform classes such as deeply incised valleys, upper slopes and high ridges show significant similarity between TOPO and ASTER, whereas landforms like headwaters, plains, open slopes and local ridges are better defined by SRTM. However, in delineation of shallow valleys and mid-slope ridges, both SRTM and ASTER are equally competent. In PRB, ASTER shows better capability for delineation of deeply incised valleys, whereas SRTM has a better delineation capability for open slope, upper slope, local ridge and mid-slope ridge. However, in defining high ridges, ASTER and SRTM data are equally reliable with respect to TOPO.

5.2.10. Hypsometric analysis

Hypsometric analysis is the study of the distribution of ground surface area, or horizontal cross-sectional area, of a landmass with respect to elevation (Strahler, 1952). The hypsometric curve (Langbein, 1947) is a non-dimensional area-elevation relationship which allows ready comparison of catchments and is traditionally associated with different stages of catchment maturity (Strahler, 1964). Hypsometric integral (I_{hyp}) is a dimensionless measure (expresses in %) of the subsurface volume of a drainage basin, referred to the 100 percent value given by "a solid bounded on the sides by the vertical projection of the basin perimeter and on the top and base by parallel planes passing through the summit and mouth respectively" (Strahler, 1952). I_{hyp} is an indicator of the remnant of the present volume in comparison with the original volume of the basin (Ritter et al., 2002), thus helps in explaining the erosion that had taken place in the watershed during the geological time scale due to fluvial and hillslope processes (Bishop et al., 2002).

The I_{hyp} of MRB derived from TOPO is 51.46 (Suppl Tables), whereas that of ASTER, SRTM and GMTED are 53.29, 52.31 and 52.05 respectively. Similarly, I_{hyp} of PRB generated from TOPO is 47.67, while ASTER, SRTM and GMTED have the values 47.85, 47.79 and 47.54 respectively. The I_{hyp} (Strahler, 1952) implies a late youth to early mature stage of geomorphic development of MRB and PRB. Another classification by Willgoose and Hancock (1998) differentiates basins with $I_{hyp} > 0.5$ as catchments dominated by diffusive erosion processes (hillslope) and values <0.5 dominated by fluvial erosion processes. The hypsometric curves generated from various DEMs of MRB and PRB are given in Fig. 7c and d and the hypsometric curve geometry of different spaceborne DEMs in MRB and PRB are analogous with TOPO.

5.2.11. Stream network analysis

Wang and Yin (1998) suggested stream-length and -frequency as significant proxies manifesting the integrity of the DEM-derived drainage networks. Hence, in this study, the aforementioned parameters are considered for the comparison of stream network extracted from the DEMs and the results are given in Table 2.

In MRB, the drainage networks of TOPO and GMTED have more or less similar number of streams of different orders, whereas SRTM and ASTER show considerable variation (Table 2). Comparison of number of streams of different stream orders between TOPO and ASTER reveals that third order streams have the maximum variability, followed by second order streams (Fig. 8a). But in case of SRTM, second order shows maximum variability with respect to TOPO. However, the total number of streams of TOPO and SRTM are exactly same (i.e., 135), while GMTED and ASTER show comparatively smaller numbers (129 and 123 respectively). At the same time, in PRB, ASTER gives better similarity in the order-wise as well as total number of streams with that of TOPO, whereas SRTM and GMTED have significant differences (Table 2). All the DEMs (except ASTER) show maximum deviation in second order streams of PRB followed by third order (Fig. 8b).

In MRB, the total length of streams extracted from TOPO is relatively higher (218.06 km; Table 2), compared to ASTER (206.19 km), SRTM (204.96 km) and GMTED (203.26 km). Even though the total stream length in PRB derived from TOPO (236.80 km) is also comparably higher than other DEMs (226.73, 228.16 and 221.54 for ASTER, SRTM and GMTED respectively), the variation is relatively smaller compared to MRB. Moreover, among various stream orders, third order shows larger deviation of stream length in both the basins (Fig. 8c and d). In addition, in MRB, total length of second order streams also has significant variability among the DEMs.

Bifurcation ratio (Rb), one of the network composition parameters (Strahler, 1958), represents the structural organization of the drainage network. Since there is a close similarity on the number of streams between TOPO and GMTED in MRB, there is hardly any noticeable variation of Rb between successive orders (Table 2; Fig. 8a). Further, mean Rb derived from the DEMs does not show any large variations, but in general, SRTM (Rb = 4.85) has a better agreement (instead of GMTED, Rb = 4.74) with TOPO (Rb = 4.83). However, in PRB, ASTER has significantly comparable mean Rb compared to TOPO (Table 2; Fig. 8b), while Rb derived from SRTM and GMTED shows remarkable deviation. The stream length ratio (Rl) of MRB derived from the DEMs shows wider range of values (Table 2; Fig. 8c) and SRTM has the closer value (Rl = 3.95) compared to TOPO (5.20). Rl derived from ASTER and GMTED is relatively smaller (2.81 and 3.36 respectively) and the variation is an outcome of difference in the order-wise length of streams. In PRB, the variation in mean Rl among the different DEMs is relatively smaller (Table 2; Fig. 8d) compared to MRB and SRTM has a comparable Rl (4.64) with TOPO (4.21). Though mean Rl of ASTER is relatively larger (4.87), Rl between lower stream orders shows better similarity with TOPO (Table 2; Fig. 8d). On comparison, there is only a very small variation in the drainage density (Dd) of MRB and PRB derived from different DEMs (Table 2).

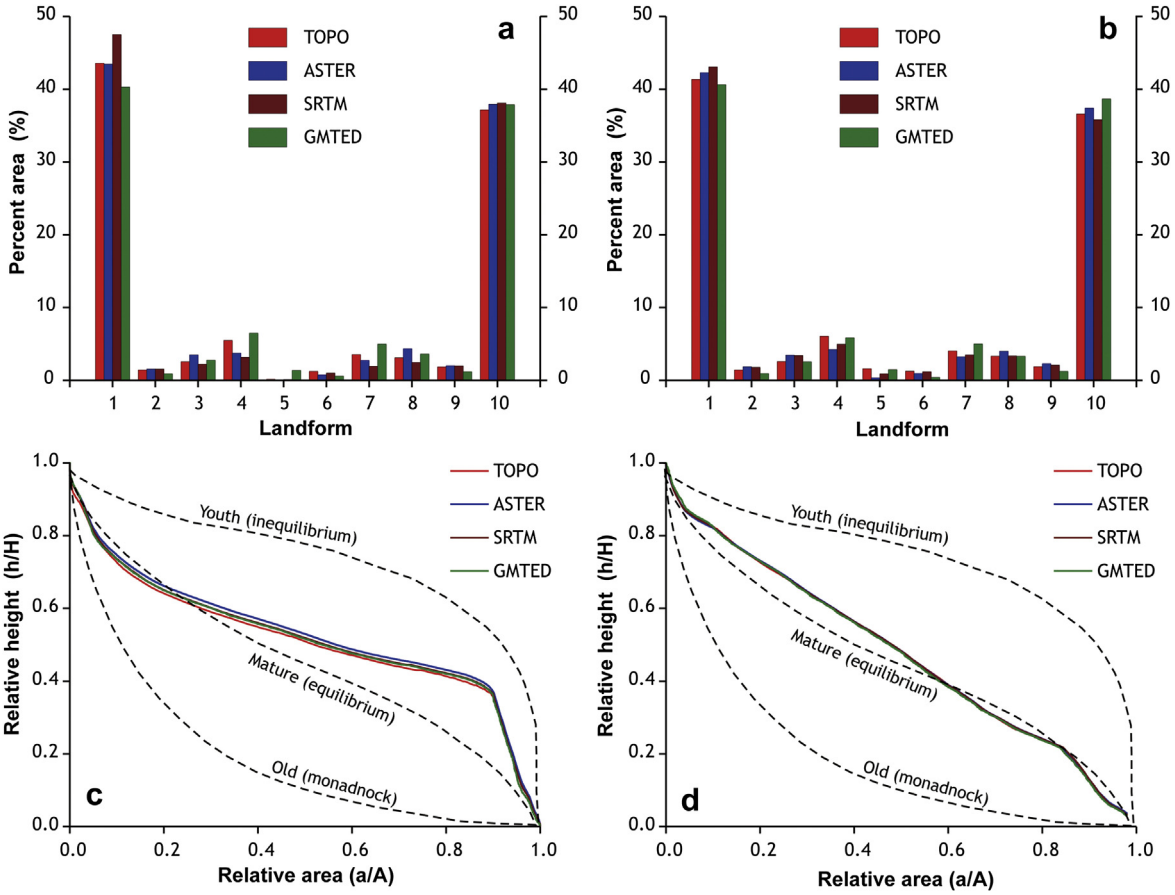

Figure 7. Areal coverage of various landforms (a, b) and hypsometric curves (c, d) of MRB and PRB respectively.

6. Discussion and conclusion

The mountainous terrain of the southern Western Ghats has a decisive role in determining the climate, vegetation and hydrologic characteristics of west-flowing rivers in Kerala. Further, the unique topography and landforms of the region, significantly controlling various environmental variables, such as climate, channel morphology, vegetation, weathering pattern, soil properties, are

Table 2
Comparison of stream network parameters of MRB and PRB extracted from various DEMs.

Parameter	MRB				PRB			
	TOPO	ASTER	SRTM	GMTED	TOPO	ASTER	SRTM	GMTED
N1	106	97	100	100	111	112	104	102
N2	22	21	27	22	30	29	21	23
N3	6	4	7	6	8	8	6	7
N4	1	1	1	1	1	1	1	1
ΣNT	135	123	135	129	150	150	132	133
L1 (km)	1.08	1.18	1.05	1.10	1.06	0.99	1.14	1.14
L2 (km)	2.71	2.12	1.63	2.45	2.33	2.41	3.29	2.86
L3 (km)	2.44	6.08	3.71	3.13	2.83	2.40	2.51	2.11
L4 (km)	29.77	22.94	29.80	20.64	26.16	26.80	25.82	24.89
LT1 (km)	114.14	114.41	105.08	110.00	118.11	110.88	118.15	116.13
LT2 (km)	59.51	44.52	44.08	53.82	69.86	69.86	69.11	65.74
LT3 (km)	14.64	24.32	26.00	18.80	22.67	19.19	15.08	14.78
LT4 (km)	29.77	22.94	29.80	20.64	26.16	26.80	25.82	24.89
ΣLT (km)	218.06	206.19	204.96	203.26	236.80	226.73	228.16	221.54
Rb_{1-2}	4.82	4.62	3.70	4.55	3.70	3.86	4.95	4.43
Rb_{2-3}	3.67	5.25	3.86	3.67	3.75	3.63	3.50	3.29
Rb_{3-4}	6.00	4.00	7.00	6.00	8.00	8.00	6.00	7.00
Rb_{mean}	4.83	4.62	4.85	4.74	5.15	5.16	4.82	4.91
Rl_{2-1}	2.51	1.80	1.55	2.22	2.19	2.43	2.90	2.51
Rl_{3-2}	0.90	2.87	2.28	1.28	1.22	1.00	0.76	0.74
Rl_{4-3}	12.20	3.77	8.02	6.59	9.23	11.17	10.27	11.79
Rl_{mean}	5.20	2.81	3.95	3.36	4.21	4.87	4.64	5.01
Dd	0.80	0.75	0.75	0.76	0.82	0.79	0.77	0.79

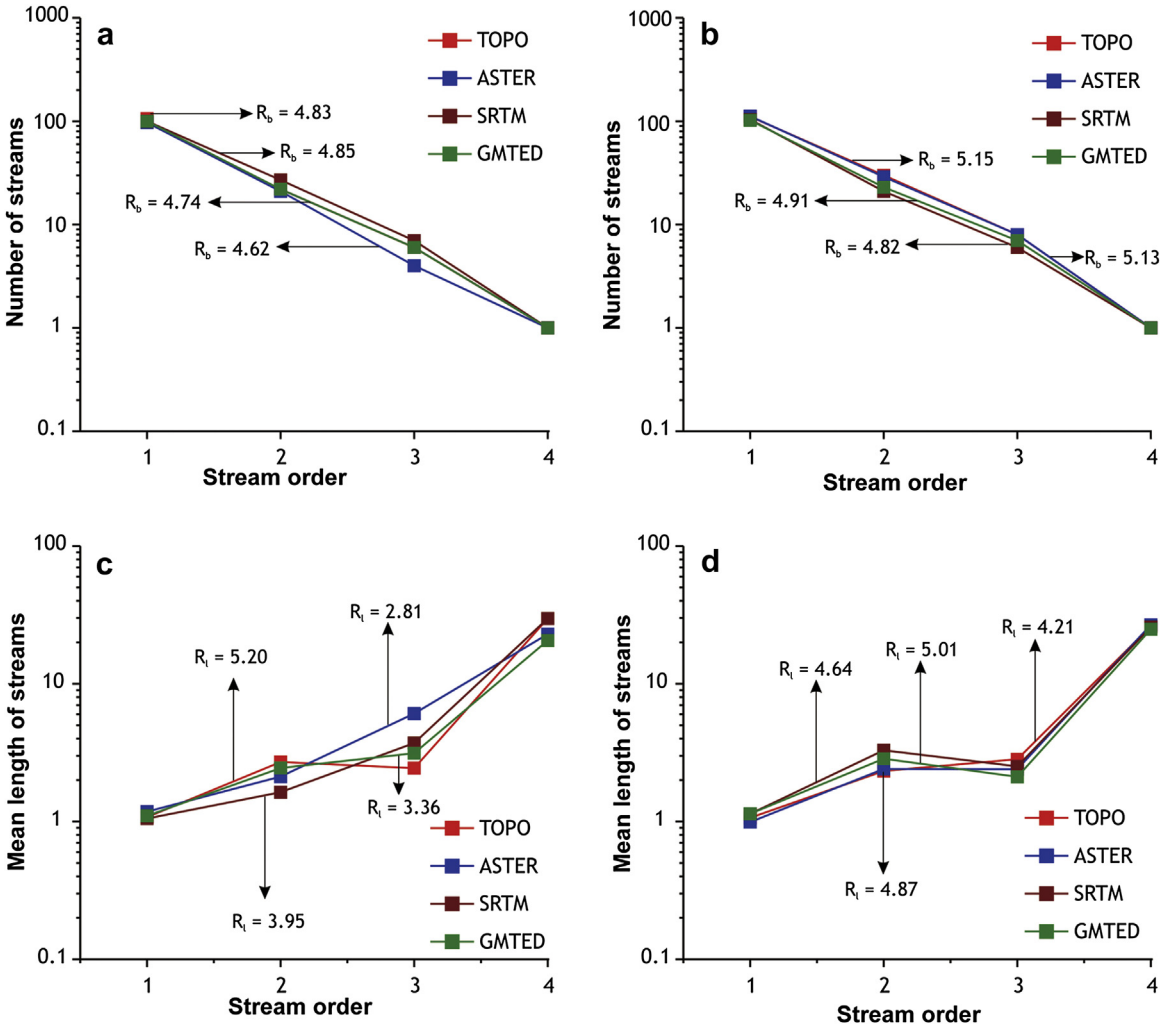

Figure 8. Horton's laws of stream number (a, b) and stream length and (c, d) of MRB and PRB respectively.

highly sensitive to various natural as well as anthropogenic factors (Thomas, 2012). However, in tropical mountain river basins, except a few studies (e.g., Prasannakumar et al., 2011; Kia et al., 2012; Yamazaki et al., 2012; Zani et al., 2012), application of spaceborne DEMs for geomorphometric and hydrologic applications as well as terrain characterization is limited.

Among ASTER, SRTM and GMTED DEMs, SRTM has relatively lower MAE and RMSE, implying relatively higher vertical accuracy, while GMTED shows comparably lower level of accuracy, which is a result of coarser spatial resolution compared to other DEMs. In order to assess the influence of terrain relief on vertical accuracy of the spaceborne DEMs, DEM error statistics (MAE and RMSE) in different relative relief classes (e.g, <200, 200–400 and >400 m/km^2) are estimated (Table 3). In both MRB and PRB, MAE and RMSE of all the spaceborne DEMs are relatively lower in areas of lower relative relief (i.e., <200 m/km^2) and DEM errors are higher in areas of higher relative relief (>400 m/km^2). In MRB, the range of MAE of lower relief areas for ASTER, SRTM and GMTED is 20.00–35.33, 10.00–25.00 and 31.50–67.00 respectively, while RMSEs for ASTER, SRTM and GMTED are 21.83–42.08, 10.46–29.55 and 36.54–86.75 respectively (Table 3). Similarly, in PRB, the areas of lower relief show comparatively lower range of error statistics, i.e., ASTER (MAE = 8.50–32.40; RMSE = 9.16–33.12), SRTM (MAE = 9.83–26.10; RMSE = 10.86–27.68) and GMTED (MAE = 33.17–58.30; RMSE = 33.78–62.09). In general, the magnitude of MAE and RMSE in areas of higher relative relief is almost two to three times as that in areas of lower relief. Such dependency of DEMs on terrain complexity is observed by several researchers (e.g., Gorokhovich and Voustianiouk, 2006; Shortridge and Messina, 2011; Jing et al., 2013; Li et al., 2013).

Similarly, to assess the impact of land use types on vertical accuracy, estimated DEM error statistics (MAE and RMSE) are grouped according to various land use types. Three major types of land use are selected in MRB (forest, Eucalyptus plantation and open scrub) and PRB (forest, open scrub and farmland) and DEM error statistics of each land use types are given in Table 4. In MRB, relatively higher MAE and RMSE for ASTER (32.59 and 38.26 respectively), SRTM (21.59 and 26.52) and GMTED (55.41 and 69.57) are observed over forested areas (Table 4), while lower MAE and RMSE are associated with open scrub (i.e., grasses and smaller shrubs). Similarly, in PRB, higher MAE and RMSE are noticed over forested areas, e.g., ASTER (25.50 and 28.84 respectively), SRTM (20.70 and 24.60) and GMTED (50.90 and 55.16), whereas lower error statistics are observed over farmlands (except MAE of SRTM and GMTED). Several studies (e.g., Sun et al., 2003; Chirico et al., 2012; Jing et al., 2013) also suggested that the accuracy of spaceborne DEMs over forested areas is relatively lower than that in other land use types, especially in farmlands and built-up areas.

In general, SRTM provides better vertical accuracy in both basins, reaffirming the observations of Kaab (2005) and Huggel et al.

Table 3
Error statistics of various DEMs with respect to relative relief, MRB and PRB.

Relative relief (m/km^2)	MRB								PRB							
	MAE				RMSE				MAE				RMSE			
	TOPO	ASTER	SRTM	GMTED	TOPO	ASTER	SRTM	GMTED	TOPO	ASTER	SRTM	GMTED	TOPO	ASTER	SRTM	GMTED
<200	10.00	20.00	10.00	31.50	11.07	21.83	10.46	36.54	5.17	8.50	9.83	33.17	6.15	9.16	10.86	33.78
200–400	8.06	26.94	18.61	43.39	9.54	31.75	22.51	50.99	9.58	17.58	12.83	37.17	10.34	19.26	15.88	40.49
>400	7.50	35.33	25.00	67.00	8.11	42.08	29.55	86.75	9.40	32.40	26.10	58.30	10.36	33.12	27.68	62.09

(2008) that SRTM provides better vertical accuracy in spite of the coarser spatial resolution and suggesting the efficacy of InSAR DEMs over DEMS derived by digital photogrammetry of stereo pairs. However, in low relief areas of PRB, ASTER also shows relatively lower error statistics. SRTM and ASTER show relatively higher elevation in most of the sampled locations compared to the reference elevation. In a comparison of SRTM and ASTER DEMs for a subtropical hilly landscape in southeastern China, Jing et al. (2013) observed an overestimation of elevation for SRTM and ASTER DEMs. SRTM and ASTER DEMs differ in their production techniques/generation process in that SRTM is an InSAR DEM, while ASTER is generated using 3N (nadir-viewing) and 3B (backward-viewing) bands by digital photogrammetry. Obviously, overestimation of radar DEMs is predictable since radar signal returns are affected by vegetation cover (Guth, 2006; Shortridge, 2006). Rodriguez et al. (2005) and Nelson et al. (2009) suggested that SRTM data of mountainous areas is susceptible to problems due to foreshortening and shadowing. Since radar-based DEMs (i.e., SRTM) contain lot of speckling (noise) and features (such as towers or mountains) can be mislocated due to a foreshortening effect whereby features that are tilted towards the direction of the radar signal are compressed and thereby shadowing (Nelson et al., 2009). Kaab (2005) reported that terrain sections that are problematic for the SRTM (e.g., steep slopes and sharp peaks) are often problematic for photogrammetric DEM (e.g., ASTER) too. The photogrammetric DEMs will also have spikes or pits in places where the DEM generating algorithm incorrectly matches two points from the stereopair. In addition, the effect of vegetation canopies gives higher elevation values, rough surfaces and higher slope values (Nelson et al., 2009). Slater et al. (2011) suggested that the orbital characteristics of the Terra spacecraft might also have an influence on ASTER elevation data. However, Mukherjee et al. (2013) reported that ASTER DEM provides slightly more accuracy (in Shiwalik Himalaya) compared to SRTM, which is attributed to the relatively finer spatial resolution of ASTER DEM.

Between the basins, MRB has relatively higher MAE and RMSE and the attribution is to the differences in the relief pattern (Fig. 5c,d) and vegetation characteristics (i.e., densely-vegetated MRB of humid climate vs. sparsely-vegetated PRB of semi-arid climate). The MAE and RMSE of all the spaceborne DEMs over the forested land use in MRB are numerically larger than that in PRB (Table 4). Even though MRB and PRB have forest land use, southern montane wet temperate forests, west coast tropical evergreen forests and southern sub-tropical hill forests dominate MRB, whereas PRB is mainly composed of southern montane wet temperate forests, southern tropical thorn forests, southern dry mixed deciduous forests and southern moist mixed deciduous forests. Further, southern tropical thorn forests and southern dry mixed deciduous forests, dominating PRB, are relatively shorter with thin canopy cover and sparsely distributed. However, west coast tropical evergreen forests and southern sub-tropical hill forests in MRB are composed with relatively taller trees with denser canopy cover. In addition, occurrence of forest in areas of comparatively higher relative relief might increase the DEM errors due to the synergic effect of terrain complexity and land use. Reuter et al. (2009) suggested that the radar DEMs represent the true terrain in areas where the canopy cover of a forest is not dense or the vegetation is short and with small leaves and branches, which is true for PRB.

In both basins, SRTM has relatively better precision in elevation data defining the basin statistics and the spatial variability across the basins compared to ASTER and GMTED. In respect of various topographic derivatives, SRTM and ASTER generate adequately acceptable results in comparison with TOPO. However, spatial correlation of various topographic attributes between TOPO and spaceborne DEMs are essential to address the spatial quality of the DEMs. Hence, Pearson's correlation analysis is applied to measure the strength of relationships among various topographic attributes derived from the DEMs (Kienzle, 2004). Since TOPO is taken as the reference DEM, selected topographic attributes (e.g., elevation, relative relief, slope, plan and profile curvature, LS factor, TRI and TWI) of ASTER, SRTM and GMTED are compared with those derived from TOPO (Table 5). In general, relatively larger correlation coefficients for elevation, relative relief, slope and TRI imply stronger spatial correlation, whereas plan- and profile-curvature, LS factor and TWI show poor correlation (i.e., practically non-existent relationships). Among the DEMs, SRTM shows better spatial relationship with TOPO, whereas the relationship between GMTED and TOPO is relatively weaker except for elevation, relative relief and TRI. In addition, PRB shows comparably larger correlation coefficients for all the topographic attributes in comparison with MRB.

In landform characterization, ASTER and SRTM show varying precision for different landform units. For example, open slopes and local ridges are delineated by SRTM with significant precision, whereas ASTER has a better capability to extract deeply incised valleys. In both MRB and PRB, most of the landforms delineated by SRTM and ASTER show hardly any significant differences in comparison

Table 4
Error statistics of various DEMs with respect to various land use types, MRB and PRB.

Land use	MRB								PRB							
	MAE				RMSE				MAE				RMSE			
	TOPO	ASTER	SRTM	GMTED	TOPO	ASTER	SRTM	GMTED	TOPO	ASTER	SRTM	GMTED	TOPO	ASTER	SRTM	GMTED
Forest	7.18	32.59	21.59	55.41	8.15	38.26	26.52	69.57	9.10	25.50	20.70	50.90	10.45	28.44	24.60	55.16
Eucalyptus	7.50	24.50	17.25	36.00	9.14	27.49	18.79	39.27	–	–	–	–	–	–	–	–
Open Scrub	9.83	17.00	10.67	29.83	10.81	19.31	11.55	33.93	8.21	18.07	14.14	40.21	8.95	20.63	16.81	44.73
Farmland	–	–	–	–	–	–	–	–	9.00	15.67	15.00	42.33	10.34	17.46	16.42	43.97

Table 5
Pearson correlation coefficients for topographic attributes estimated from TOPO vs. other DEMs, MRB and PRB.

Attribute	MRB			PRB		
	ASTER	SRTM	GMTED	ASTER	SRTM	GMTED
Elevation	0.983	0.988	0.969	0.992	0.995	0.981
Relative relief	0.855	0.880	0.745	0.897	0.902	0.773
Slope	0.702	0.759	0.410	0.774	0.803	0.473
Plan curvature	0.244	0.321	0.140	0.283	0.354	0.169
Profile curvature	0.352	0.424	0.255	0.371	0.447	0.282
LS factor	0.358	0.416	0.237	0.476	0.488	0.250
TRI	0.839	0.864	0.766	0.902	0.910	0.804
TWI	0.281	0.305	0.106	0.358	0.393	0.122

All the correlations are statistically significant at 0.01 level (2-tailed).

with that of TOPO. The stream network attributes predominantly indicating network topology and network geometry generated from ASTER and SRTM show significant differences in both the basins, which could be attributed to varying spatial resolutions. The stream characteristics of MRB (mostly developed on Munnar Plateau) are remarkably outlined by SRTM, whereas ASTER shows significant deviation. On the other hand, in PRB (developed on the plateau scarps), ASTER defined the drainage properties more precisely, while SRTM exhibits relatively higher variability (except for mean Rl).

Even though GMTED has a comparable elevation data with TOPO, ASTER and SRTM, larger spatial resolution (i.e., 250 m) incapacitates GMTED to represent the complex topography of these mountainous basins, which manifest as the overestimation of various geomorphometric attributes. Further, the variability of hydrologic parameters, viz., TWI and stream network attributes derived from GMTED shows a noticeable difference between MRB and PRB in that variation of Rb and Rl between successive stream orders in MRB has a close agreement with that of TOPO, whereas in PRB, these parameters have significant deviations. Moreover, such variability in the attributes might be a result of contrasting terrain setting between the basins.

In summary, among various spaceborne DEMs (ASTER, SRTM and GMTED), SRTM and ASTER elevation datasets provide equally reliable representation of actual topography portrayed by TOPO and hence a valid source of topographic information that can be retrieved in relatively shorter span of time and are useful in catchment-scale hydrologic as well as geomorphologic investigations.

Acknowledgments

The first author is indebted to late Dr. R. Satheesh (SES, Mahatma Gandhi University, Kerala) for motivating in mountain research. Dr. V. Prasannakumar, Director, IUCGIST, University of Kerala is also thankfully acknowledged for the facilities and support for GIS analysis. Financial support from Kerala State Council for Science, Technology, and Environment, Thiruvananthapuram and permission for the field studies in the protected areas by Kerala Forest Department are also delightedly acknowledged. The authors gratefully acknowledge the anonymous reviewers and editors for constructive comments and suggestions.

Appendix A. Supplementary data

Supplementary data related to this article can be found at http://dx.doi.org/10.1016/j.gsf.2013.12.008

References

Aguilar, F.J., Aguera, F., Aguilar, M.A., Carvajal, F., 2005. Effects of terrain morphology, sampling density, and interpolation methods on grid DEM accuracy. Photogrammetric engineering and remote sensing 71 (7), 805–816.

Amundsen, R., Harden, J.W., Singer, M.J., 1994. Factors of soil formation: a fiftieth anniversary perspective. Soil Science Society of America Journal Special publication 33.

Beasom, S.L., Wiggers, E.P., Giardino, J.R., 1983. A technique for assessing land surface ruggedness. Journal of Wildlife Management 47 (4), 1163–1166.

Bennie, J., Huntley, B., Wiltshire, A., Hill, M.O., Baxter, R., 2008. Slope, aspect and climate: spatially explicit and implicit models of topographic microclimate in chalk grassland. Ecological Modelling 216 (1), 47–59.

Beven, K.J., Kirkby, M.J., 1979. A physically based, variable contributing area model of basin hydrology. Hydrological Sciences Bulletin 24 (1), 43–69.

Bishop, M.P., Shroder, J.F., Bonk, R., Olsenholler, J., 2002. Geomorphic change in high mountains: a western Himalayan perspective. Global and Planetary Change 32 (4), 311–329.

Burt, T.P., Butcher, D.P., 1985. Topographic control of soil moisture distributions. Journal of Soil Science 36 (3), 469–486.

Chaplot, V., Darboux, F., Bourennane, H., Leguedois, S., Silvera, N., Phachomphon, K., 2006. Accuracy of interpolation techniques for the derivation of digital elevation models in relation to landform types and data density. Geomorphology 77 (1–2), 126–141.

Chapman, C.A., 1952. A new quantitative method of topographic analysis. American Journal of Science 250 (6), 428–452.

Chen, Z.S., Hsieh, C.F., Jiang, F.Y., Hsieh, T.H., Sun, I.F., 1997. Relations of soil properties to topography and vegetation in a subtropical rain forest in southern Taiwan. Plant Ecology 132 (2), 229–241.

Chirico, P.G., Malpeli, K.C., Trimble, S.M., 2012. Evaluation of an ASTER-derived global digital elevation model (GDEM) version 1 and version 2 for two sites in western Africa. GIScience & Remote Sensing 49 (6), 775–801. http://dx.doi.org/10.2747/1548-1603.49.6.775.

Danielson, J.J., Gesch, D.B., 2011. Global Multi-resolution Terrain Elevation Data 2010 (GMTED2010). US Geo-logical Survey, p. 26. Open-File Report 2011–1073.

Darnell, A.R., Barclay, J., Herd, R.A., Phillips, J.C., Lovett, A.A., Cole, P., 2012. Geographical information system approaches for hazard mapping of dilute lahars on Montserrat, West Indies. Bulletin of Volcanology 74 (6), 1337–1353. http://dx.doi.org/10.1007/s00445-012-0596-y.

de Vente, J., Poesen, J., Govers, G., Boix-Fayos, C., 2009. The implications of data selection for regional erosion and sediment yield modelling. Earth Surface Processes and Landforms 34 (15), 1994–2007. http://dx.doi.org/10.1002/esp.1884.

Elmahdy, S.I., Mostafa Mohamed, M., 2013. Remote sensing and GIS applications of surface and near-surface hydromorphological features in Darfur region, Sudan. International Journal of Remote Sensing 34 (13), 4715–4735. http://dx.doi.org/10.1080/01431161.2013.781287.

Fabricius, C., Coetzee, K., 1992. Geographic information systems and artificial intelligence for predicting the presence or absence of mountain reedbuck. South African Journal of Wildlife Research 22 (3), 80–86.

Farr, T.G., Rosen, P.A., Caro, E., Crippen, R., Duren, R., Hensley, S., Kobrick, M., Paller, M., Rodriguez, E., Roth, L., Seal, D., Shaffer, S., Shimada, J., Umland, J., Werner, M., Oskin, M., Burbank, D., Alsdorf, D., 2007. The shuttle radar topography mission. Reviews of Geophysics 45 (2), RG2004. http://dx.doi.org/10.1029/2005RG000183.

Florinsky, I.V., 1998a. Accuracy of local topographic variables derived from digital elevation models. International Journal of Geographical Information Science 12 (1), 47–62.

Florinsky, I.V., Kuryakova, G.A., 1996. Influence of topography on some vegetation cover properties. Catena 27 (2), 123–141.

Gallant, J.C., Wilson, J.P., 2000. Primary topographic attributes. In: Wilson, J.P., Gallant, J.C. (Eds.), Terrain Analysis: Principles and Applications. John Wiley and Sons, New York, pp. 51–96.

Gandolfi, C., Bischetti, G.B., 1997. Influence of the drainage network identification method on geomorphological properties and hydrological response. Hydrological Processes 11 (4), 353–375.

Gorokhovich, Y., Voustianiouk, A., 2006. Accuracy assessment of the processed SRTM-based elevation data by CGIAR using field data from USA and Thailand and its relation to the terrain characteristics. Remote Sensing of Environment 104 (4), 409–415. http://dx.doi.org/10.1016/j.rse.2006.05.012.

Greenwalt, C.R., Shultz, M.E., 1962. Principals of Error Theory and Cartographic Applications. Technical Report No. 96. Aeronautical Chart and Information Center, St. Louis, Missouri.
Gunnell, Y., Radhakrishna, B.P. (Eds.), 2001. Sahyadri: The Great Escarpment of the Indian Subcontinent, vol. 47. Geological Society of India, Bangalore. Memoir.
Guth, P.L., 2006. Geomorphometry from SRTM: comparison to NED. Photogrammetric Engineering and Remote sensing 72 (3), 269–277.
Hirt, C., Filmer, M.S., Featherstone, W.E., 2010. Comparison and validation of the recent freely-available ASTER-GDEM ver1, SRTM ver4.1 and GEODATA DEM-9S ver3 digital elevation models over Australia. Australian Journal of Earth Sciences 57 (3), 337–347.
Hjerdt, K.N., McDonnell, J.J., Seibert, J., Rodhe, A., 2004. A new topographic index to quantify downslope controls on local drainage. Water Resources Research 40 (5), W05602. http://dx.doi.org/10.1029/2004WR003130.
Horton, R.E., 1945. Erosional development of streams and their drainage basins: hydrophysical approach to quantitative morphology. Geological Society of America Bulletin 56 (3), 275–370.
Huggel, C., Schneider, D., Miranda, P.J., Granados, H.D., Kaab, A., 2008. Evaluation of ASTER and SRTM DEM data for lahar modeling: a case study on lahars from Popocatepetl Volcano, Mexico. Journal of Volcanology and Geothermal Research 170 (1–2), 99–110.
Jarvis, A., Reuter, H.I., Neson, A., Guevara, E., 2008. Hole-filled SRTM for the Globe Version 4. http://srtm.csi.cgiar.org.
Jayappa, K.S., Markose, V.J., Nagaraju, M., 2012. Identification of geomorphic signatures of neotectonic activity using DEM in the Precambrian Terrain of Western Ghats, India. In: International Archives of the Photogrammetry, Remote Sensing and Spatial Information Sciences, vol. XXXIX-B8. XXII ISPRS Congress, 25 August – 01 September 2012, Melbourne, Australia.
Jenness, J., 2006. Topographic Position Index (tpi_jen.avx) Extension for ArcView 3.x, v. 1.2. Jenness Enterprises. Available at: http://www.jennessent.com/arcview/tpi.htm.
Jenny, H., 1941. Factors of Soil Formation. McGraw Hill, New York.
Jing, C., Shortridge, A., Lin, S., Wu, J., 2013. Comparison and validation of SRTM and ASTER GDEM for a subtropical landscape in Southeastern China. International Journal of Digital Earth. http://dx.doi.org/10.1080/17538947.2013.807307.
Johnson, C.E., Ruiz-Mendez, J.J., Lawrence, G.B., 2000. Forest soil chemistry and terrain attributes in a catskills watershed. Soil Science Society of America Journal 64 (5), 1804–1814.
Kaab, A., 2005. Combination of SRTM3 and repeat ASTER data for deriving alpine glacier flow velocities in the Bhutan Himalaya. Remote Sensing of Environment 94 (4), 463–474.
Kale, V.S., Shejwalkar, N., 2007. Western Ghats escarpment evolution in the Deccan Basalt Province: geomorphic observations based on DEM Analysis. Journal of the Geological Society of India 70, 459–473.
Kale, V.S., Shejwalkar, N., 2008. Uplift along the western margin of the Deccan Basalt Province: is there any geomorphometric evidence? Journal of Earth System Science 117 (6), 959–971.
Kervyn, M., Ernst, G.G.J., Goossens, R., Jacobs, P., 2008. Mapping volcano topography with remote sensing: ASTER vs. SRTM. International Journal of Remote Sensing 29 (22), 6515–6538.
Kia, M.B., Pirasteh, S., Pradhan, B., Mahmud, A.R., Sulaiman, W.N.A., Moradi, A., 2012. An artificial neural network model for flood simulation using GIS: Johor River Basin, Malaysia. Environmental Earth Sciences 67 (1), 251–264. http://dx.doi.org/10.1007/s12665-011-1504-z.
Kienzle, S., 2004. The effect of DEM raster resolution on first order, second order and compound terrain derivatives. Transactions in GIS 8 (1), 83–111.
Koehler, G.M., Hornocker, M.G., 1989. Influences of season on bobcats in Idaho, USA. Journal of Wildlife Management 53 (1), 197–202.
Langbein, W.B., 1947. Topographic Characteristics of Drainage Basins. US Geological Society Water Supply Paper 968C, Washington DC.
Li, P., Shi, C., Li, Z., Muller, J.P., Drummond, J., Li, X., Li, T., Li, Y., Liu, J., 2013. Evaluation of ASTER GDEM using GPS benchmarks and SRTM in China. International Journal of Remote Sensing 34 (5), 1744–1771. http://dx.doi.org/10.1080/01431161.2012.726752.
Lopez, C., 1997. Locating some types of random errors in digital terrain models. International Journal of Geographical Information Science 11 (7), 677–698.
Magesh, N.S., Chandrasekar, N., Soundranayagam, J.P., 2011. Morphometric evaluation of Papanasam and Manimuthar watersheds, parts of Western Ghats, Tirunelveli district, Tamil Nadu, India: a GIS approach. Environmental Earth Sciences 64 (2), 373–381.
Magesh, N.S., Jitheshlal, K.V., Chandrasekar, N., Jini, K.V., 2013. Geographical information system-based morphometric analysis of Bharathapuzha river basin, Kerala, India. Applied Water Science 3 (2), 467–477. http://dx.doi.org/10.1007/s13201-013-0095-0.
Merritt, W.S., Letcher, R.A., Jakeman, A.J., 2003. A review of erosion and sediment transport models. Environmental Modelling & Software 18 (8–9), 761–799.
Miller, C.L., Laflamme, R.A., 1958. The digital terrain model: theory and application. Photogrammetric Engineering 24, 433.
Moore, I.D., Burch, G.J., 1986a. Physical basis of the length-slope factor in the Universal Soil Loss Equation. Soil Science Society of America Journal 50 (5), 1294–1298.
Moore, I.D., Burch, G.J., 1986b. Modeling erosion and deposition: topographic effects. Transactions of the American Society of Agricultural and Biological Engineers 29 (6), 1624–1630.
Moore, I.D., Gesseler, P.E., Nielsen, G.A., Peterson, G.A., 1993. Soil attribute prediction using terrain analysis. Soil Science Society of America Journal 57 (2), 443–452.
Moore, I.D., Grayson, R.B., Ladson, A.R., 1992. Digital terrain modelling: a review of hydrological, geomorphological, and biological applications. In: Beven, K.J., Moore, I.D. (Eds.), Terrain Analysis and Distributed Modelling in Hydrology. Wiley, New York, pp. 7–34.
Moore, I.D., Wilson, J.P., 1992. Length-slope factors for the revised universal soil loss equation: simplified method of estimation. Journal of Soil and Water Conservation 47 (5), 423–428.
Mouratidis, A., Briole, P., Katsambalos, K., 2010. SRTM 3" DEM (version 1, 2, 3, 4) validation by means of extensive kinematic GPS measurements: a case study from North Greece. International Journal of Remote Sensing 31 (23), 6205–6222.
Mukherjee, S., Joshi, P.K., Mukherjee, S., Ghosh, A., Garg, R.D., Mukhopadhyay, A., 2013. Evaluation of vertical accuracy of open source Digital Elevation Model (DEM). International Journal of Applied Earth Observation and Geoinformation 21, 205–217. http://dx.doi.org/10.1016/j.jag.2012.09.004.
Nellemann, C., Fry, G., 1995. Quantitative analysis of terrain ruggedness in reindeer winter grounds. Arctic 48 (2), 172–176.
Nelson, A., Reuter, H.I., Gessler, P., 2009. DEM production methods and sources. In: Hengl, T., Reuter, H.I. (Eds.), Geomorphometry: Concepts, Software, Applications. Elsevier, Oxford, pp. 65–86.
Nikolakopoulos, K.G., Kamaratakis, E.K., Chrysoulakis, N., 2006. SRTM vs. ASTER elevation products: comparison for two regions in Crete, Greece. International Journal of Remote Sensing 27 (21), 4819–4838.
Ollier, C.D., 1990. Mountains. In: Barto-Kyriakidis, A. (Ed.), Critical Aspects of the Plate Tectonic Theory vol. 2. Theophrastus, Athens, pp. 211–236.
Pike, R.J., Wilson, S.E., 1971. Elevation-relief ratio, hypsometric integral and geomorphic area-altitude analysis. Geological Society of America Bulletin 82 (4), 1079–1084.
Prasannakumar, V., Shiny, R., Geetha, N., Vijith, H., 2011. Applicability of SRTM data for landform characterisation and geomorphometry: a comparison with contour-derived parameters. International Journal of Digital Earth 4 (5), 387–401.
Pryde, J.K., Osorio, J., Wolfe, M.L., Heatwole, C., Benham, B., Cardenas, A., June 2007. Comparison of watershed boundaries derived from SRTM and ASTER digital elevation datasets and from a digitized topographic map. Paper No. 072093. In: ASABE Meeting, pp. 17–20 (Minneapolis, MN).
Quinn, P.F., Beven, K.J., Lamb, R., 1995. The ln (a/tanβ) index: how to calculate it and how to use it within the TOPMODEL framework. Hydrological Processes 9 (2), 161–182.
Quinn, P.F., Beven, K.J., 1993. Spatial and temporal predictions of soil moisture dynamics, runoff, variable source areas and evapotranspiration of Plynlimon, Mid-Wales. Hydrological Processes 7 (4), 425–448.
Rabus, B., Eineder, M., Roth, A., Bamler, R., 2003. The Shuttle Radar Topography Mission: a new class of digital elevation models acquired by spaceborne radar. ISPRS Journal of Photogrammetry and Remote Sensing 57 (4), 241–262.
Renard, K.G., Foster, G.A., Weesies, D.A., McCool, D.K., Yoder, D.C., 1997. Predicting Soil Erosion by Water: A Guide to Conservation Planning with the Revised Universal Soil Loss Equation (RUSLE). USDA Agriculture Handbook 703, Washington DC.
Renfrew, R.B., Ribic, C.A., 2002. Influence of topography on density of grassland passerines in pastures. American Midland Naturalist 147 (2), 315–325.
Renschler, C.S., Harbor, J., 2002. Soil erosion assessment tools from point to regional scales – the role of geomorphologists in land management research and implementation. Geomorphology 47 (2–4), 189–209.
Reuter, H.I., Hengl, T., Gessler, P., Soille, P., 2009. Preparation of DEMs for geomorphometric analysis. In: Hengl, T., Reuter, H.I. (Eds.), Geomorphometry: Concepts, Software, Applications. Elsevier, Oxford, pp. 87–120.
Reuter, H.I., Nelson, A., 2009. Geomorphometry in ESRI packages. In: Hengl, T., Reuter, H.I. (Eds.), Geomorphometry: Concepts, Software, Applications. Elsevier, Oxford, pp. 269–291.
Riley, S.J., DeGloria, S.D., Elliot, R., 1999. A terrain ruggedness index that quantifies topographic heterogeneity. Intermountain Journal of Sciences 5 (1–4), 23–27.
Ritter, D.F., Kochel, R.C., Miller, J.R., 2002. Process Geomorphology. McGraw Hill, Boston.
Rodriguez, E., Morris, C.S., Belz, J.E., 2006. A global assessment of the SRTM performance. Photogrammetric Engineering and Remote Sensing 72 (3), 249–260.
Rodriguez, E., Morris, C.S., Belz, J.E., Chapin, E.C., Martin, J.M., Daffer, W., Hensley, S., 2005. An Assessment of the SRTM Topographic Products. Jet Propulsion Laboratory, Pasadena, California, 143 pp.
Seibert, J., Stendahl, J., Sorensen, R., 2007. Topographical influences on soil properties in boreal forests. Geoderma 141 (1–2), 139–148.
Sharma, A., Tiwari, K.N., Bhadoria, P.B.S., 2010. Vertical accuracy of digital elevation model from Shuttle Radar Topographic Mission: a case study. Geocarto International 25 (4), 257–267.
Shinde, V.M., Deshpande, P.K., Kumthekar, M.B., 2013. Application of ASTER DEM in watershed management as flood zonation mapping in Koyana River of the Western Ghats. International Journal of Scientific & Engineering Research 4 (5), 297–301.
Shortridge, A., 2006. Shuttle radar topography mission elevation data error and its relationship to land cover. Cartography and Geographic Information Science 33 (1), 65–75. http://dx.doi.org/10.1559/152304006777323172.

Shortridge, A., Messina, J., 2011. Spatial structure and landscape associations of SRTM error. Remote Sensing of Environment 115 (6), 1576–1587. http://dx.doi.org/10.1016/j.rse.2011.02.017.
Singh, P., Kumar, N., 1997. Effect of orography on precipitation in the western Himalayan region. Journal of Hydrology 199 (1–2), 183–206.
Singh, P., Ramasastri, K.S., Kumar, N., 1995. Topographical influence on precipitation distribution in different ranges of Western Himalayas. Nordic Hydrology 26 (4–5), 259–284.
Slater, J.A., Garvey, G., Johnston, C., Haase, J., Heady, B., Kroenung, G., Little, J., 2006. The SRTM data 'finishing' process and products. Photogrammetric Engineering and Remote Sensing 72 (3), 237–247.
Slater, J.A., Heady, B., Kroenung, G., Curtis, W., Haase, J., Hoegemann, D., Shockley, C., Tracy, K., 2011. Global assessment of the new ASTER global digital elevation model. Photogrammetric Engineering and Remote sensing 77 (4), 335–349.
Soman, K., 2002. Geology of Kerala. Geological Society of India, Bangalore.
Strahler, A.N., 1952. Hypsometric (area-altitude) analysis of erosional topography. Geological Society of America Bulletin 63 (11), 1117–1142.
Strahler, A.N., 1957. Quantitative analysis of watershed geomorphology. Transactions of American Geophysical Union 38 (6), 913–920.
Strahler, A.N., 1958. Dimensional analysis applied to fluvially eroded landforms. Geological Society of America Bulletin 69 (3), 279–300.
Strahler, A.N., 1964. Quantitative geomorphology of drainage basins and channel networks. In: Chow, V.T. (Ed.), Handbook of Applied Hydrology. McGraw Hill, New York, pp. 4-39–4-76.
Sun, G., Ranson, K.J., Kharuk, V.I., Kovacs, K., 2003. Validation of surface height from shuttle radar topography mission using shuttle laser altimeter. Remote Sensing of Environment 88 (4), 401–411.
Suwandana, E., Kawamura, K., Sakuno, Y., Kustiyanto, E., 2012. Thematic information content assessment of the ASTER GDEM: a case study of watershed delineation in West Java, Indonesia. Remote Sensing Letters 3 (5), 423–432.
Tarboton, D.G., Bras, R.L., Rodrigues-Iturbe, I., 1992. On the extraction of channel networks from digital elevation data. In: Beven, K.J., Moore, I.D. (Eds.), Terrain Analysis and Distributed Modelling in Hydrology. Wiley, New York, pp. 85–104.
Thomas, J., 2012. Channel characteristics of two upland river basins of contrasting climate: a study from Kerala. Ph.D. Thesis. University of Kerala, Thiruvananthapuram, Kerala, India.
Thomas, J., Joseph, S., Thrivikramji, K.P., 2010. Morphometric aspects of a small tropical mountain river system, the southern Western Ghats, India. International Journal of Digital Earth 3 (2), 135–156.
Thomas, J., Joseph, S., Thrivikramji, K.P., Abe, G., 2011. Morphometric analysis of the drainage system and its hydrological implications in the rain shadow regions, Kerala, India. Journal of Geographical Sciences 21 (6), 1077–1088.
Thomas, J., Joseph, S., Thrivikramji, K.P., Abe, G., Kannan, N., 2012. Morphometrical analysis of two tropical mountain river basins of contrasting environmental settings, the southern Western Ghats, India. Environmental Earth Sciences 66 (8), 2353–2366.
Thompson, J.A., Bell, J.C., Butler, C.A., 2001. Digital elevation model resolution: effects on terrain attribute calculation and quantitative soil-landscape modeling. Geoderma 100 (1–2), 67–89.
Toutin, T., 2008. ASTER DEMs for geomatic and geoscientific applications: a review. International Journal of Remote Sensing 29 (7), 1855–1875.
USGS, 1998. Standards for Digital Elevation Models, Part 3, Quality Control, National Mapping Program Technical Instructions. United States Geological Survey. Retrieved from. http://nationalmap.gov/standards/demstds.html.
Vaze, J., Teng, J., Spencer, G., 2010. Impact of DEM accuracy and resolution on topographic indices. Environmental Modelling & Software 25 (10), 1086–1098. http://dx.doi.org/10.1016/j.envsoft.2010.03.014.
Wang, X., Yin, Z.-Y., 1998. A comparison of drainage networks derived from digital elevation models at two scales. Journal of Hydrology 210 (1–4), 221–241.
Weiss, A., 2001. Topographic Position and Landform Analysis. Poster Presentation, ESRI User Conference, San Diego, California.
Western, A.W., Grayson, R.B., Bloschl, G., Willgoose, G.R., McMahon, T.A., 1999. Observed spatial organization of soil moisture and its relation to terrain indices. Water Resources Research 35 (3), 797–810.
Willgoose, G., Hancock, G., 1998. Revisiting the hypsometric curve as an indicator of form and process in transport-limited catchment. Earth Surface Processes and Landforms 23 (7), 611–623.
Wilson, J.P., Gallant, J.C., 2000. Digital terrain analysis. In: Wilson, J.P., Gallant, J.C. (Eds.), Terrain Analysis: Principles and Applications. John Wiley and Sons, New York, pp. 1–28.
Wischmeier, W.H., Smith, D.D., 1978. Prediction Rainfall Erosion Losses: A Guide to Conservation. USDA Agricultural Handbook 537, Washington DC.
Wu, S., Li, J., Huang, G.H., 2008. A study on DEM-derived primary topographic attributes for hydrologic applications: sensitivity to elevation data resolution. Applied Geography 28 (3), 210–223.
Yamazaki, D., Baugh, C.A., Bates, P.D., Kanae, S., Alsdorf, D.E., Oki, T., 2012. Adjustment of a spaceborne DEM for use in floodplain hydrodynamic modeling. Journal of Hydrology 436–437, 81–91. http://dx.doi.org/10.1016/j.jhydrol.2012.02.045.
Zani, H., Assine, M.L., McGlue, M.M., 2012. Remote sensing analysis of depositional landforms in alluvial settings: method development and application to the Taquari megafan, Pantanal (Brazil). Geomorphology 161–162, 82–92. http://dx.doi.org/10.1016/j.geomorph.2012.04.003.
Zebker, H.A., Goldstein, R.M., 1986. Topographic mapping from interferometric synthetic aperture radar observations. Journal of Geophysical Research: Solid Earth 91 (B5), 4993–4999.
Zevenbergen, L.W., Thorne, C.R., 1987. Quantitative analysis of land surface topography. Earth Surface Processes and Landforms 12 (1), 47–56.
Zinko, U., Seibert, J., Dynesius, M., Nilsson, C., 2005. Plant species numbers predicted by a topography-based groundwater flow index. Ecosystems 8 (4), 430–441.